Winter 12-15-2019

A Microfluidic Platform to Investigate the Mechanism by which GDNF Overexpression in Schwann Cells Causes Neuronal Axon Entrapment

Ze Zhong Wang
Washington University in St. Louis

WASHINGTON UNIVERSITY IN ST. LOUIS

McKelvey School of Engineering

Department of Biomedical Engineering

Dissertation Examination Committee:
Dennis Barbour, Chair
Shelly Sakiyama-Elbert, Co-Chair
Paul Bridgman
Daniel Moran
Jonathan Silva
Matthew Wood

A Microfluidic Platform to Investigate the Mechanism by which GDNF Overexpression in Schwann Cells Causes Neuronal Axon Entrapment

By

Ze Zhong Wang

A dissertation presented to
The Graduate School
of Washington University in
partial fulfillment of the
requirements for the degree
of Doctor of Philosophy

December 2019
Saint Louis, Missouri

Table of Contents

List of Figures

List of Tables

Acknowledgments

First, I would like to thank Shelly Sakiyama-Elbert, my advisor, for all your guidance and mentoring. I have truly learned so much from you on the disciplines of scientific research. Although I am far from being a good researcher, you have shown me the necessary skillsets to become one. For the past 6 years, your guidance has gradually helped me develop my own understanding and approach for solving scientific problems. I surely will continue to benefit from your mentorship for years to come. Thank you again for your patience and wonderful guidance.

I would also like to thank my co-workers in the Sakiyama-Elbert Lab. To Jennifer Pardieck, Russell Thompson, Nick White, Nisha Iyer, Thomas Wilems, Hao Xu, Laura Marquardt, Michael Saunders, and Jaewon Lee, thank you all for your companionship. Coming to the lab was such a pleasant experience for me everyday because you are always there to help, listen, talk, and enjoy a good laugh with. To Sara Oswald, you have welcomed me to the family at the start of my Ph.D journal. You were always there to solve our crises and always there to cheer me up. To Mary Salazar, thank you for alleviating us from the endless but necessary ordering of supplies, which ensured our research progress was never delayed.

I would like to thank Dr. Susan Mackinnon and her lab. Especially, I would like to thank Matthew Wood. Your help was critical in forming my research endeavors. I also want to thank Xueping Ee. You have offered tremendous support for providing and culturing Schwann cells. I am grateful for all of your help.

I would like to thank my thesis committee members: Dennis Barbour, Paul Bridgman, Jonathan Silva, Danial Moran, and Matthew Wood. Thank you for your time and guidance

throughout my thesis work. I would also like to acknowledge my funding sources from National Institutes of Health.

I would like to thank all my friends in St. Louis, Austin, San Diego, Vancouver, and Changchun. Finally, I would like to thank my family. My parents, you have never failed to support me on whatever decisions I want to make. You have always been there for me to talk about all my problems. I am fortunate to be your son. I would also like to thank my loving wife Julia for her support through most of my Ph.D career. Thank you for you understanding and sacrifice.

Ze Zhong Wang

Washington University in St. Louis

December 2019

To my parents, my wife Julia, and my child to be. Without your support and encouragement, none of this would have been possible.

ABSTRACT OF DISSERTATION

A Microfluidic Platform to Investigate the Mechanism by which GDNF Overexpression in Schwann Cells Causes Neuronal Axon Entrapment

By Ze Zhong (Bill) Wang

Doctor of Philosophy in Biomedical Engineering

Washington University in St. Louis, 2019

Professor Dennis Barbour, Chair

Professor Shelly Sakiyama-Elbert, Co-Chair

Twenty million Americans suffer from peripheral nerve injury (PNI) caused by trauma and medical disorders, with approximately $150 billion spent in annual health-care dollars in the United States. Even with proper surgical reconstruction, less than 50% of the patients achieve satisfactory functional recovery. The gold standard surgical repair for long gaps (>3cm) is the autologous nerve graft, despite its disadvantages such as donor site morbidity, risk of infection, and increased cost. Alternative methods, such as acellular nerve grafts (ANA), are ineffective for large lesion gaps because of the lack of cells and regeneration factors. Recent efforts have been focused on the application of exogenous growth factors, based on their roles during development and post-injury. Of particular interest for this study, following PNI, the distal nerve and denervated muscles increase expression of glial cell line-derived neurotrophic factor (GDNF) to stimulate axonal growth. However, the duration of this response is often insufficient to promote the full reinnervation of end-organ targets, especially for large injury gaps. To extend the period of release of GDNF, our lab has previously engineered transgenic SCs with constitutive overexpression of GDNF (G-SCs). However, we and others have also discovered that such constitutive GDNF

overexpression causes axon entrapment in vivo. Specifically, regenerating axons fail to extend beyond the GDNF source and form dense nerve coils at the site of overexpression, a phenomenon termed the "candy-store" effect. The mechanism by which GDNF overexpression causes the "candy-store" effect is unclear. Moreover, the complexity of the in vivo environment presents a major challenge to effectively study the "candy-store" effect. Therefore, in this dissertation, we developed a microfluidic platform to model axon entrapment *in vitro* and studied the mechanism by which high levels of GDNF can cause the "candy-store" effect.

First, we recapitulated neuronal axon entrapment using dissociated chicken embryonic dorsal root ganglion (DRGs) in a 3-chamber microfluidic device. Consistent with *in vivo* results, G-SCs were able to cause axon entrapment in this platform. Importantly, we found that a high concentration of soluble GDNF (700ng/mL) is sufficient to induce axon entrapment. In addition, axon entrapment caused by high GDNF concentration cannot be overcome by distal sources of high GDNF levels. To further investigate the underlying mechanism, we used DNA microarray to identify differentially expressed genes in neurons treated with high GDNF. Slitrk4 was upregulated by high GDNF treatment, and the knockdowns of Slitrk4 resulted in reduced axon entrapment. Similar to the effects of soluble GDNF, G-SCs resulted in non-reversible axon entrapment that cannot be overcome by distal sources of high GDNF levels. We also examined the effects of SCs preconditioned with high GDNF on neurite extension. While high GDNF preconditioned SCs also induced axon entrapment, such effect was reversible when distal sources of high GDNF levels were present. Together, our results have highlighted the mechanism by which GDNF can cause neuronal axon entrapment and may contribute to developing drug delivery strategies that harness only the beneficial effects of GDNF while avoiding the negative impact.

Chapter 1: Introduction

1.1 Overview

This work seeks to understand the effects of glial cell-line derived neurotrophic factor (GDNF) in high concentrations on axon growth and Schwann cell (SC) *in vitro*. SCs are glia in the peripheral nervous system (PNS) that are involved in axon guidance, growth, and myelination. More importantly, they are critical for axon regeneration following peripheral nerve injury (PNI). Patients suffering from proximal injuries are less likely to recover, as regenerating axons need to travel long distances (that takes an extended time) to reconnect to the end-organ targets [1]. This chronic denervation can cause neuronal apoptosis and SC atrophy, both of which severely impede axon regeneration [2]. Following PNI, the SCs in the distal nerve and denervated muscles increase the expression of GDNF to stimulate axonal growth [3]. However, the duration of this response is often insufficient to promote the full reinnervation of end-organ targets, especially for large gap injury [4]. To extend the period of GDNF expression, our lab has previously engineered transgenic SCs to constitutively overexpress GDNF (G-SCs) [5,6]. However, we and others have also found that constitutive GDNF overexpression causes axon entrapment *in vivo* [7,8]. Specifically, regenerating axons fail to extend beyond the GDNF source and form dense nerve coils at the site of overexpression, a phenomenon termed the "candy-store" effect [8,9]. The mechanism by which GDNF overexpression causes the "candy-store" effect is unclear. Moreover, the complexity of the *in vivo* environment presents a major challenge to effectively study the "candy-store" effect. The current thesis aimed to understand the underlying mechanisms of how GDNF can affect axonal regeneration and impact the growth-promoting ability of SCs to induce axon entrapment. This work aimed to recapitulate the "candy-store" effect *in vitro* by first developing an *in vitro* culture

platform using a 3-chamber microfluidic device. The underlying mechanism by which GDNF causes the axon entrapment was also investigated.

The first part of this work focused on modeling the "candy-store" effect *in vitro*. Studying the "candy-store" effect *in vivo* can be difficult, given the complexity of the environment and involvement of multiple cell types in the PNS. Standard *in vitro* culture systems also lack the means to separate neuronal soma from axons for effectively studying the causes of axon entrapment. An *in vitro* model system was created to recapitulate axon entrapment using a 3-chamber microfluidic device. The device consists of three culture chambers (somal, middle, and distal) connected by microchannels that prevent cell somas from moving between chambers while allowing neurites to grow between chambers. Since the G-SCs overexpress GDNF, neurons were cultured under high GDNF concentrations to model axon entrapment. Soft lithography was used to fabricate the microfluidic device. Axon entrapment was evaluated based on the number of axons that fail to extend beyond the middle chamber.

The second focus of this thesis is centered on understanding the mechanism by which high GDNF levels directly affect neurons and also impact the growth-promoting ability of SCs to induce axon entrapment. Previous work suggests that axon entrapment is mediated either directly by high GDNF concentrations and/or SCs that are affected by high GDNF concentration. Exposing SCs to a physiological level of GDNF (preconditioned SCs, 100 ng/mL) promotes axon growth. In contrast, G-SCs, which express a supra-physiological level of GDNF, induce axon entrapment. In addition, DNA microarray data indicates that G-SCs have a distinct gene expression profile compared to normal SCs and SCs preconditioned with GDNF. By using the microfluidic device designed in the previous study, SCs pretreated with physiological and supra-physiological concentrations of GDNF or G-SCs were cultured in the middle chamber. Axon growth was

assessed under these conditions to evaluate the impact on axons crossing the middle chamber toward the distal chamber. To understand the effects of different levels of GDNF on neurons, we used DNA microarrays to reveal potential gene targets related to axon entrapment. In addition, RNA interference was used on the target genes to investigate their role in entrapment induced by GDNF.

The following introduction will highlight the characteristics and biology of PNI, the role of SCs in promoting peripheral nerve regeneration, and the importance of growth factors in enhancing this process. More importantly, the use of GDNF on peripheral nerve regeneration and its limitations will be discussed. Current treatment strategies will also be discussed.

1.2 Peripheral Nerve Injury

PNS is one of two branches of the nervous systems. Whereas the central nervous system (CNS) includes the brain and the spinal cord, the PNS extends outside the CNS and serves to control the movement of the limb as well as providing sensory feedback to the CNS. PNI caused by trauma and medical disorders affects twenty million Americans, incurring a cost of approximately $150 billion in healthcare [10,11]. It was estimated that PNI constitutes as 2-3% of all patients admitted to a Level I trauma center, and can be as high as 5% when plexus and nerve root injuries are included [12,13]. Damage to the PNS can result in impaired motor and/or sensory nerve function and denervated end-organs. While the PNS has greater inherent capabilities for regeneration compared with the CNS, the regeneration process faces many challenges that can greatly limit functional recovery of patients and severe nerve injury often has a devastating impact on a patient's quality of life. This section will describe PNI and regeneration as well as the challenges for functional recovery.

1.1.1 Neurobiology of Peripheral Nerve Injury and Regeneration

Many factors, including the patient's age, the delay before surgical intervention, and the type of injury, affect the recovery of PNI. The most common causes of PNIs are laceration, crush, and nerve stretch injuries [14,15]. In the upper limb extremity, radial, ulnar, and median nerve injuries are the most common [12]. Sciatic, peroneal and tibial/femoral are the most common in the lower limb [16]. In general, patients suffering from complete transection of nerves are less likely to recover than from crush injuries. More importantly, the proximity of the injury to the nerve cell body can greatly impact the degree of recovery. Distal injuries, such as sensory loss to a fingertip, can often regenerate well. In comparison, proximal brachial plexus avulsions, where the injury site is close to the cell body, often result in poor recovery with limited hand sensation and reduced motor function.

Following injury, molecular and cellular changes occur at different levels of the PNS. At the neuron soma, the withdrawal of trophic support from target organs can significantly influence neuronal survival. Critical transcriptional changes occur, which will determine whether to induce apoptosis or promote regeneration in neurons [17]. The incidence of apoptosis-related cell death in dorsal root ganglion neurons following axonotmesis ranges from 20 to 50% [18,19]. Distal segments of the nerve to the injury site also experience profound molecular and cellular changes, a phenomenon known as Wallerian degeneration (WD). This process allows for the distal nerve segment to be prepared for regenerating axons by clearing distal axon segments and myelin debris [20,21]. Within a few hours after injury, both the axon and the myelin in the distal stump degenerate [22]. One of the key components that distinguish the PNS from the CNS is the ability of Schwann cells (SC) to assist this degeneration process. Myelin debris is inhibitory to regenerating axons (as in the CNS). In the first 24hr, the denervated SCs de-differentiate into an immature state that

proliferate and migrate towards the site of axon and myelin breakdown. With the combined actions of SCs and macrophages, inhibitory debris is removed [23]. SCs then align in the remaining basal lamina and endoneurial tubes to form the bands of Bungner. These structures are formed when the SCs lay down extracellular matrix (ECM) and organize into columnar tracks for regenerating axons to follow[24,25]. At the same time, SCs begin to upregulate surface proteins, such as neural cell adhesion molecules (NCAM), and secrete neurotrophic proteins, such as nerve growth factor (NGF), brain-derived neurotrophic factor (BDNF), and glial cell-line derived neurotrophic factor (GDNF) [26,27]. Additional trophic support is also provided by the end target organs, such as muscles and skin [28]. After migrating through the endoneurial tubes, the axons are myelinated by SCs and reestablish connections with target end-organs. Correct reinnervation of the end-organ signals that the axons are fully matured.

1.1.2 Challenges in Peripheral Nerve Regeneration

Several major challenges can hinder functional recovery in the PNS. One of the critical barriers caused by proximal injuries is chronic denervation. Since axons may take months to years to cross long injury gaps (>2cm), chronic denervation causes SCs and target tissue to atrophy. SCs stop maintaining bands of Bungner, and the basal lamina also degenerate and disappear [29]. In addition to these changes, SCs lose their ability to provide trophic support and become inefficient at promoting axon growth [30,31]. Similarly, target organs also experience atrophy due to chronic denervation. Noticeable decreases in the number and size of muscle fibers, along with increases in fibrosis are observed [32]. Even when reinnervation of the muscle eventually occurs, full functional recovery of muscles is rarely observed. In animal models of chronic denervation, regenerated axons were observed to be near target muscles. However, these axons have minimal branching and failed to form synapses, suggesting that the muscles are no longer receptive to innervation by axons

[33]. Another obstacle caused by proximal injury is chronic axotomy where the axons lost contact with the target tissue for an extended time. Both sensory and motor neuron showed significant decreases in number after chronic denervation [19,34].

Even when axons can eventually reach target organs, the regenerating axons may incorrectly reinnervate the wrong end-organ target. The disruption of endoneurial tubes can lead to inappropriate reinnervation, where motor axons may reinnervate sensory organs and vice versa [35,36]. If a functionally unrelated end organ is reached, further development of the axon and remyelination do not occur. Another issue with reinnervation occurs when cross-reinnervation occurs even when a sufficient number of motor axons reach the muscles. Erroneous cross-reinnervation may result in an originally "fast" muscle reinnervated by axons previously innervating "slow" muscle, and the result may be a mixed form with inefficient contraction [22]. Overall, there remain many challenges facing axonal regeneration and functional recovery. Chronic denervation and chronic axotomy reduce the growth potential of neurons, SCs, and target organs. Even with sufficient axon growth, functional recovery could be impaired by incorrect reinnervation. Therefore, to design adequate therapies to promote correct axonal regeneration, all of these factors need to be considered.

1.2 PNI Treatment Strategies

1.2.1 Nerve Repair Using Biological Grafts

Different repair strategies are used based on the severity and type of PNI. For injuries that require surgical intervention, direct nerve repair with epineural microsutures is performed when a tension-free coaptation in a well-vascularized bed can be achieved [2]. This technique lines up both the internal nerve fascicles and the surface epineural blood vessel patterns, thus achieving gross fascicular matching between the proximal and distal nerve ends. Another technique involves

grouped fascicular repair and direct matching and suturing of the fascicles. However, more trauma and scarring offset the advantages of better fascicle alignment with this approach. Functional outcomes using group fascicular repair is not better than epineural repair [18]. The difficulties with direct nerve repair include reproducing the original alignment of nerve fascicles and minimizing tension. One requirement for direct repair is removing entire damaged nerve segment to prevent scar formation, which inhibits regeneration, and revealing the normal fascicular pattern for regenerating axons to maintain alignment across the coaptation [37,38]. For injuries that require extensive tissue remove, end-to-end coaptation could cause longitudinal tension, which can result in chronic ischemia and damage to the endoneurial structure [39,40].

When a tension-free primary repair is not possible, nerve grafts can be used to bridge injury gaps. Commonly used grafts include autologous nerve graft (autograft) and acellular nerve allograft (ANA). Autograft is considered the gold standard for bridging long injury gaps (>3cm), more proximal injuries, and critical nerves [41]. Similar to joining distal nerve segment in direct repair, autografts provide a permissive and stimulating scaffold, including Schwann cells, basal laminae, neurotrophic factors, and adhesion molecules [39]. Since donor nerves are harvested from patients, the autografts are also nonimmunogenic compared to cadaveric nerve allografts. The choice of autograft depends on the size of the nerve gap, location of the proposed nerve repair, and associated donor-site morbidity [37]. The sural nerve from the leg is the most commonly used donor nerve. Other nerves that are also harvested include the medial antebrachial cutaneous nerve, the lateral antebrachial cutaneous nerve, dorsal cutaneous branch of the ulnar nerve, superficial and deep peroneal nerves, intercostal nerves, and the posterior and lateral cutaneous nerves of the thigh [42,43]. Even though autograft is the clinical standard of repair for long injury gaps, it presents several major drawbacks. First, the size of the autograft is limited. Studies showed that trunk grafts from

a large nerve could result in central necrosis and fibrosis due to inadequate vascularization [44,45]. Also, the donor graft and the repaired nerve need to match in the diameter and number of fibers. Small sensory nerves are less effective than phenotype matched motor grafts in promoting regeneration in large diameter motor nerves [46,47]. Another cause for inefficient regeneration also stems from matching sensory grafts with motor branches. Because sensory loss is preferred over the motor deficit, sensory nerves are usually sacrificed. However, motor regenerating axons show preferential motor reinnervation, a process in which motor axons will preferentially reinnervate muscle over skin [48]. This process makes sensory grafts less desirable for repairing motor function. Other complications of autografts include donor site morbidity leading to sensory loss, neuroma formation, and the need for a second incision to harvest donor nerve.

As an alternative strategy, cadaveric nerve allografts present several advantages over autografts. Compared to autografts, cadaver supply is more plentiful than autografts. In addition, there is no donor site morbidity. It also eliminates the need for second surgeries to harvest donor nerves, which may result in complications. In clinical practice, allografts have been used to successfully repair nerve gaps up to 70 mm [49]. Although nerve allografts are a potential alternative to autografts, immunogenicity must be considered. SCs and myelin within allografts can elicit host rejection, thereby necessitating concurrent immunosuppression for up to two years [2]. Until host SCs can completely replace and populate the donor nerve, donor SCs have to act as support cells for remyelination. However, donor SCs are also the major contributor to immunogenicity as they are the primary sources of major histocompatibility complex II molecules [50]. This drawback led to strategies to reduce immunogenicity.

Several techniques have been developed to reduce allograft immunogenicity leading to the development of acellular nerve allograft (ANA). In particular, decellularization of allogeneic nerve

reduces immunogenicity by eliminating antigenic factors, such as Schwann cells and myelin, while retaining the natural basement membrane and three-dimensional ECM to guide axonal regeneration [51,52]. Common strategies include cryopreservation and detergent decellularization. Cryopreservation involves cold preservation of the graft in the University of Wisconsin Cold Storage Solution at 5°C for seven days, which will preserve the basal lamina and laminin distribution [53]. Viability of the SCs also decreased with increasing time of cold storage. As a result, immune response and graft rejection were decreased, and regeneration was increased. Combined with FK-506, which has been demonstrated to augment axon regeneration, cryopreservation has produced reliable and robust clinical outcomes [54–56]. An alternative strategy for decellularization is to use detergent. Using amphoteric detergents sulfobetaine (SB)-10 and SB-16, and an anionic detergent, Triton X-200, Hudson *et al.* found that optimized antigen removal protocol that causes minimal damage to the ECM and basement membrane [57]. In a 14-mm rat sciatic nerve injury model, Moore *et al.* showed that detergent-processed allograft promoted axon regeneration and muscle force similar to isograft and superior to both the commercially available ANA, AxoGen and cryopreserved allograft [58]. Even though ANA offers as an alternative to autografts for short injury gaps (<3cm), they are not effective for gaps greater than 4 cm [59]. Therefore, alternative strategies for repairing long gap injuries must be developed.

1.2.2 Nerve Guidance Conduits

Recent research has been focusing on developing nerve guidance conduits (NGC). The most studied material for NGCs is collagen. Commercially available NGCs are composed of collagen type I, III, or IV. It can be used as both a conduit material as well as a luminal filler. It is important to recognize the effects of collagen on different cell types to better design NGCs. In the PNS, collagen trimers are essential for basal lamina ECM assembly, which is critical for SCs

maturation and myelination [60–62]. *In vitro* studies showed that various types of collagen seem to have different effects on cells. For instance, α4 Type V collagen promoted SC adhesion and migration but inhibited dorsal root ganglion neurite outgrowth [63,64]. Upon further examination, it was shown that the collagen domain of Type V blocked neurite outgrowth, while the non-collagen N-terminal domain improved neurite outgrowth as well as promoting SC migration. These findings highlight the importance of using different collagen types and derivatives for different purposes and cell types. Using a combination of the right collagen and matching cells might significantly impact the regenerative potential of the collagen scaffold. Currently, bovine collagen Type I is the primary collagen type used in FDA-approved nerve conduits, such as NeuraGen®, NeuroFlex™, and NeuraWrap™. In particular, NeuraGen has been extensively studied and used in clinical settings [65,66]. Mackinnon *et al.* conducted the first trials using collagen-based material showing no occurrence of compression neuropathy in comparison with other more rigid or silicon materials in a [65]. A later study compared the effectiveness of collagen-based conduit to autograft and direct suturing in repairing 4mm gap in rat and non-human primate nerves [66]. The results show that by 12 weeks, the collagen-based conduits showed similar recovery to autografts and direct suturing. Later clinical studies also demonstrated the use of NeuraGen in patients with injury gaps $\leq$ 2cm [67]. Analysis of 126 repairs in 96 patients that received NeuraGen showed minimal complications and sensory recovery in the 35%-45% range. Compared with autografts, collagen-based conduits are abundant. They also represent little immunogenicity. However, one major drawback of collagen-based conduits is batch-to-batch variations can compromise reproducible performance.

Synthetic NGCs are gaining more attention in recent years. Synthetic polymers, such as poly(glycolic acid) (PGA), poly(lactic acid) (PLA), and poly(lactic-co-glycolic acid) (PLGA), are usually synthesized to form porous scaffold fabrication due to the superior control over porosity

and pore diameters [68–71]. Synthetic polymers are also tunable and offer a great range of mechanical and physical properties, such as tensile strength, elastic modulus, and degradation rate. With defined purity and properties, these characteristics are highly reproducible. The major disadvantages of synthetic polymers, however, might be limited biocompatibility, lack of natural cell adhesion sites, cytotoxicity of solvents for fabrication, and release of toxic degradation products. Early studies on neural scaffold fabrication used non-degradable materials. Silicone was one of the most prevalent materials used. However, the silicone tube is known to cause discomfort in patients due to its rigidness [72]. Second surgeries are required to remove the silicone tubes. Currently, silicone is primarily used as an experimental model for studying PNI. Even though many positive results have been reported using non-degradable NGC, the challenges remain as non-degradable scaffold require a second surgery to remove or must be planned for permanent implantation. For PNI, non-degradable material can cause swelling and nerve compression in long-term implantation. Therefore, non-degradable materials are not the focus of current research endeavors.

PLA and PGA are two of the most extensively studied biodegradable polyester links of lactic and glycolic acid. It has been shown SCs embedded in PGA-based tissue-engineered nerve combined with pluronic F127 gel resulted in comparable numbers of regenerated axons to autograft control in 10 mm gap sciatic nerve injury in rats [68]. PGA conduits with SCs improved hind limb movements comparable to the autograft while silicone conduits showed a much lower score. It is important to note that the degradation products of PLA and PGA usually result in a lower pH of the surrounding environment, which is toxic to the cells. Another well-studied polyester is PLGA, which is a copolymer of PLA and PGA. SC transplantation in PLGA foam guides combined with glial growth factor (GGF) showed improvement on axonal regeneration and

conduction velocity in 10 mm-gap sciatic nerve injury model in rats [70]. In addition, PLGA conduit embedded with olfactory ensheathing cells (OEC) demonstrated an increase in conduction velocity of nerve fibers 16 weeks after injury, when used to repair a 15 mm-gap sciatic nerve injury in rats [73]. Transplanted OECs showed positive expression of S100β and signs of ECM deposition.

1.3 Schwann Cells

Schwann cells (SC) are the glial population of the PNS. The primary functions of SCs are myelination for large diameter axons and trophic support for small diameter axons in uninjured nerves. After injuries, SCs are responsible for removing debris from myelin and axon in distal segments of the injured nerve. They also release cytokines that will recruit macrophages to help with debris clearance. In addition, SCs release many neurotrophic factors and express cell adhesion molecules that promote axon growth. Bands of Bungner formed by SCs after injury provide structural support for regenerating axons to grow. Both providing critical functions for uninjured nerve and supporting axon regeneration after injury make studying SCs an essential task for developing therapeutics for PNI.

1.3.1 Overview of Schwann Cells

SCs originate from neural crest cells (NCCs). While the exact signaling cascade that direct NCCs towards SC lineage is unclear, Sox10 is thought to be one of the central transcription factors for generating the earliest cells in the SC lineage [74,75]. Schwann cell precursors (SCPs) are generated from migrating NCCs. Sox10 null mutant knockouts have shown development arrests prior to the generation of SC precursors (SCPs). SCPs have the potential to become immature SCs or endoneurial fibroblasts [76]. One of the most important events happening during this stage is SC-axon interaction. Unlike SCs which can survive based on autocrine signaling, SCPs depend

entirely on juxtacrine signals from axons. Neuregulin-1 (NRG1) and ErbB interactions are a critical survival factor SCP [23,77]. Absence of NRG1 not only reduced SCP survival but also negatively impact neuron survival [75,78,79]. Another important function of NRG and ErbB signaling pathway may be related to myelin formation. Knockdown of ErbB 2 results in hypomyelination of peripheral nerve [80,81]. Lack of NRG1 type III in dorsal root ganglion neurons results in defective axonal ensheathment and lack of myelination [82].

Notch signaling, being another important signaling mechanism in SC, has shown multiple roles. During development, Notch is likely acting as a maturation signal for SCPs, a mitogen for immature SCs, and an inhibitor of myelination [83]. In mice, genetic inactivation of Notch1 or the transcription factor RBPJ, which is essential for classical Notch signaling, delayed the generation of Schwann cell from precursors. Conversely, Schwann cells appear more rapidly in mice in which Notch signaling is enhanced [84]. ErbB3 receptor was upregulated, which increased the effectiveness of NRG1 signaling, suggesting the underlying mechanism may involve neuregulin. Together, these data suggest that Notching signaling help drives SCP towards SC phenotype. After injuries, Notch is upregulated to drive dedifferentiation of myelinating cells [84]. After most SCPs have converted into immature SCs, they start to envelop groups of axons, forming axon-SC columns[85]. SC proliferation and death match axon and SC numbers. Radial sorting also starts at this time, involving single axons segregating from the axon/Schwann cell families to become individually ensheathed by a Schwann cell. This is a precondition for myelination, which subsequently takes place in the case of larger axons.

SC generation is also subject to negative regulation. Endothelin has been shown to delay the appearance of immature SCs from SCPs *in vitro*[86]. *In vivo* inactivation of endothelin B receptors results in the premature appearance of immature SCs. These results suggest endothelin

acts as a negative regulator of SC generations. The transcription factor AP2a in SCPs has also been shown to play a role in the conversion of precursors to SCs [87]. Whereas AP2a is highly expressed in SCPs, its expression is dramatically decreased in immature SCs *in vivo*. This may suggest that AP2a is involved in maintaining SCP phenotype and delay the generation of SCs.

After birth, immature SCs start to generate the two distinct populations of SCs: myelinating SCs, and Remak cells. In uninjured nerves, Remak cells, or non-myelin SCs envelop all the small-diameter axons, including small nociceptive (C-type) axons, the postganglionic sympathetic axons, and the preganglionic sympathetic and parasympathetic fibers. In particular, many pre- and postganglionic axons of the autonomic nerves are unmyelinated for their entire lengths. All PNS nerves are unmyelinated for some portions of their axons and are surrounded by Remak cells. The myelinating SCs are associated with larger diameter axons. Myelin sheath formed by SC membranes can wrap multiple times around the axons resulting in insulated segments of nerve bundles. Both Remak and myelinating SCs reside within the perineurium. SCs are surrounded by a basal lamina, which is encased in the endoneurium with connective tissue, fibroblast, and blood vessels. The perineurium contains multiple endoneuriums, and the epineurium contains multiple perineuriums. Remak cells and myelinating SCs express distinct molecular profiles from each other based on their functions. Markers, such as neural adhesion molecule (NCAM), L1 adhesion molecules (L1CAM), p75 neurotrophin receptor (p75NTR), and glial fibrillary acidic protein (GFAP) are expressed in Remak cells after development. In comparison, these markers are significantly downregulated in myelin SCs after development [88]. Unique markers of the myelin SCs are associated with its primary function of myelin formation. The transcription factor early growth response 2 (ERG2/KROX20) is a major marker of myelin SCs, along with myelin protein zero (MPZ), myelin basic protein (MBP), and myelin-associated glycoprotein (MAG).

1.3.2 Repair Schwann Cell Phenotype and Its Role in Regeneration

One of the most remarkable features of SCs is their plasticity after injury. Both myelin SCs and Remak cells transform into repair-supportive SCs, which involves a series of molecular and morphological changes. In particular, myelinating SCs de-differentiate, marked by the downregulations of pro-myelin genes including Krox20, MPZ, MBP, MAG, and periaxin. Conversely, markers from immature SCs are re-expressed, including NCAM, p75NTR, GFAP, and L1 which were downregulated before birth [89–92]. The de-differentiation of SCs may suggest that repair-supportive SCs are similar to immature SCs. However, repair SCs show a unique molecular expression profile marked by the expression of GDNF, oligodendrocyte transcription factor 1 (Olig1), sonic hedgehog (Shh), and artemin [26,93]. These markers, with the exception of GDNF, are absent in immature SCs. In addition, repair SCs activate a set of repair-related genes, some of which are *de novo*. To promote neuron survival and axon regeneration, SCs release neurotrophic factors, such as GDNF, artemin, BDNF, NT-3, NGF, VEGF, erythropoietin, FGFs, pleiotrophin, and N-cadherin [26,27,94].

One of the key roles of SCs during injury is their ability to clear myelin. SCs have the ability to breakdown myelin themselves and also recruit macrophages to degrade myelin debris. During the first seven days after injury, about 50% of the myelin is degraded primarily by SCs [95]. This mechanism is important because myelin could inhibit axon growth [96,97]. Following myelin internalization, myelin is delivered to SC lysosomes for degradation [98]. Cytokines, such as interleukin-6 (Il-6) and leukemia inhibitory factor (LIF) are leased by SCs, which will recruit macrophages to the nerve [99]. Macrophages are responsible for myelin clearance after SCs. Il-6 and LIF have been shown to not only attract macrophages to the injured nerve but also act on neurons to promote axon regeneration [100]. In addition, recruited macrophages provide an additional source

of cytokines and promote vascularization of the distal nerve [95,101,102]. Morphologically, SCs undergo elongation and branching. It was shown that four weeks after injury, Remak cells increased their length by three-fold and myelin SCs doubled in length [103]. In addition, the branching of SC processes was observed lying parallel to the main axis of the cell. The elongated SCs align in columns (bands of Bungner) inside the basal lamina tubes that previously enclosed myelin and axons before injury. This structure provides essential structural support and substrate for regenerating axons to reconnect with end target organs.

Among the thousands of genes that are upregulated or downregulated, the upregulation of c-Jun plays a crucial role in SC injury response. c-Jun is activated within hours of injury and continue to increase for at least 7-10 days [103]. Knockout of c-Jun in SCs significantly compromised axon regeneration and functional recovery after sciatic nerve injury in mice [93]. In comparison, the development of SCs and nerve function in uninjured adult mice were normal. This highlight the specific expression of c-Jun during injury. With a total of approximately 4000 genes that were differentially expressed in SCs after injury, c-Jun knockout affected at least 172 genes. Among these genes, Krox20, the master regulator of myelination was no-longer downregulated, along with MPZ and MBP [93,104]. Therefore c-Jun plays a key role in helping to suppress myelin gene expression in adult nerves after injury. c-Jun is also responsible for regulating the expression of growth-promoting trophic factors. c-Jun knockout SCs failed to upregulate GDNF, artemin and BDNF, p75NTR and N-cadherin. The knockout is believed to cause more sensory neuron death in addition to initial death caused by injury [26,93]. In addition to these functions, c-Jun is also believed to affect the formation of the bands of Bungner. c-Jun knockout SCs tend to be flat and sheet-forming *in vitro* and form a disorganized structure *in vivo* after injury [93]. Recent evidence also suggests that reduced c-Jun activation is implicated in the age-dependent reduction in regeneration

in older animals [105]. Together, these findings demonstrate the importance of c-Jun expression for SC injury response.

1.4 Glial-cell Line Derived Neurotrophic Factor (GDNF)

Glial cell line-derived neurotrophic factor was originally isolated from a rat glioma cell-line as a trophic factor for the midbrain dopamine neurons. It was first found that GDNF protects dopamine neurons in animal models of Parkinson' disease [106–109]. It was also found that GDNF was involved in motor neuron survival [110]. Subsequently, GDNF has attracted a lot of attention as a potential therapeutic agent to treat neurodegenerative diseases and trauma. In addition, GDNF has important roles in other organ systems, acting as a morphogen in kidney development and regulating differentiation of spermatogonia. Ret is a single-pass transmembrane protein that contains four cadherin-like repeats in the extracellular domain and a typical intracellular tyrosine kinase domain. It was identified as a signaling receptor for GDNF. However, their interaction was of low affinity and an auxiliary ligand-binding subunit, GDNF family receptor alpha 1 (GFRα1), was identified to have high affinity with GDNF [111,112]. GFRα1 is anchored to the plasma membrane through glycosylphosphatidylinositol (GPI) anchor and does not have an intracellular domain that signals downstream pathways. Rather, it forms a complex with GDNF, which then acquires a high affinity for Ret [113]. The GDNF/GFRα1/Ret complex can then activate downstream signaling pathways, including Ras/MAP kinase and PI3K/AKT [114]. GDNF activation of the PI3K pathway is likely contributing to the neuroprotective effect of GDNF, demonstrated by the inhibition of PI3K resulted in poor motor neuron survival [115]. Chen *et al.* demonstrated that survival of sensory and motor neurons was significantly increased by intramuscular injection of GDNF. GDNF also had the most powerful effect on neurite outgrowth and elongation of sensory neuron and motor neurons compared to NGF or CNTF injections [116]. Multiple studies also demonstrated that GDNF

delivery to injured nerves could enhance functional motor recovery [117,118]. Another effect observed with subcutaneous injections of GDNF or transgenic overexpression of GDNF in skeletal muscle was hyperinnervation of neuromuscular junctions with abnormal motor endplates [119,120]. This hyperinnervation seems to counteract synapse elimination, which involves the withdrawal of the presynaptic terminal and the fine-tuning individual synaptic contacts for robust neuronal circuitry. Together, these findings suggest that GDNF offers neuron protection during the early stages of injury, promotes axon regeneration during the repair phase, and is involved in synapse formation and reinnervation of end target organs.

In addition to its effects on neurons, GDNF also showed important functions in regulating SC behavior. While GDNF signals through Ret in neurons, NCAM is likely the receptor of GDNF in SCs, along with GFRα1 as co-receptor [121]. Combined with GFR α1 and NCAM, GDNF activates Fyn, a Src family kinase, which leads to activation of the Ras-Raf and Erk1/2 pathway. This pathway regulates GDNF production by SCs, causing a positive feedback loop [122,123]. In addition, GDNF can affect SC proliferation and differentiation. Hoke *et al.* demonstrated that exogenous GDNF increased SC proliferation and induced SC myelinating phenotype of normally unmyelinated axons [124]. Findings from our lab showed that treatment of SCs with exogenous GDNF upregulates the maturation marker S100β [123]. In addition, GDNF treatment appeared to drive motor and sensory-derived SCs into their native phenotypes, which had become dysregulated with time in culture[125]. Sensory SC markers, such as MBP and BDNF, are significantly upregulated in sensory-derived SCs after GDNF treatment. Similarly, motor-derived SC markers protein kinase C iota (PRKCi) and VEGF are increased in motor-derived SCs. One of the drawbacks of using sensory-derived nerve graft, such as the sural nerve, to repair injured motor branches is that the phenotypic differences can impair recovery [46]. By pre-conditioning either motor- or sensory-

derived SCs with GDNF, our lab demonstrated that neurite extension was greatly improved in mismatch pairs of neuron and SCs to similar lengths as matched pairs [126].

1.4.1 The "Candy-Store" Effect

Studies have shown that neurotrophic factors have a very short half-life and are cleared from the body within hours [127]. Tissue penetration by diffusion is also limited [128]. Therefore, to efficiently deliver GDNF as therapeutics, we must ensure a sustained release of biologically active GDNF throughout the injury site, especially for long injury gaps. While many different delivery methods have been developed, gene therapy has shown promise in treating PNI by using lentiviral-mediated means [6,129,130]. However, one of the major drawbacks of using GDNF to improve axon regeneration is that overexpression of GDNF can cause the "candy-store" effect [8]. Axons are entrapped at the site of GDNF overexpression, and dramatic morphological changes occur in both axons and SCs. This effect was first described by Blits *et al.* where adeno-associated viral vector-mediated expressions of BDNF or GDNF were used to improve motor neuron survival after spinal ventral root avulsions in rats [8]. Both BDNF and GDNF overexpression significantly increased the number of motor neurons after injury compared to sham groups. However, analysis of the number of nerve fibers extending into the sciatic nerve for both groups were not significantly different from all other groups. In particular, GDNF-induced fiber arborization and clusters were denser at four months than that for BDNF. Using a rat sciatic nerve injury model, Santosa *et al.* demonstrated that GDNF overexpressing SCs increased the number of nerve fibers to a similar level as isograft in the midline of ANA [7]. However, this number was dramatically decreased in the distal region of the graft. Neural tissue and nerve fiber width were also significantly less than all other groups, including ANA only. Functional recovery measured by muscle force was also worse with GDNF overexpressing SCs than isograft and wildtype SCs with ANA. To bypass the negative impact of

GDNF, Eggers *et al.* attempted to establish a gradient of GDNF expression by injecting increasing dosages of lentiviral vectors with GDNF overexpression in rat sciatic nerve [130]. The "candy-store" effect was observed even with the lowest dosage of GDNF lentiviral vectors. Similar to previous studies, axons form densely pack fiber networks presented as nerve coils *in vivo* [131,132]. SC number also dramatically increased at the site of GDNF overexpression. Importantly, strong p75NTR immunoreactivity was detected, indicating the presence of immature and non-myelinating SCs. At the same time, MBP expression was decreased, and thin myelin sheath was observed. These data suggest that GDNF overexpression not only induce axon entrapment but also profoundly affect SCs morphology. Whereas moderate levels (100ng/mL) of GDNF seem to increase the expression of MBP in sensory-derived SCs, GDNF overexpression reversed such an effect [123,130].

While the exact mechanism of how GDNF causes the "candy-store" effect is unknown, our lab has previously demonstrated that temporal control of GDNF overexpression can improve regeneration while avoiding axon entrapment [6]. In a rat sciatic nerve injury model, a 3 cm injury gap was bridged by ANA containing GDNF-releasing fibrin scaffold. Tetracycline-inducible (Tet-On) GDNF overexpressing SCs were transplanted into the distal nerve to encourage growth past the ANA. It was determined that the tetracycline-induced GDNF expression for 6 weeks enabled axons to cross the 3 cm injury gap. The total number of axons detected in the distal nerve was comparable to isograft. In contrast, 4 weeks of expression was insufficient for regeneration, while 8 weeks resulted in axon entrapment. Both groups showed a significantly lower number of axons in midgraft and the distal nerve compared to isograft and 6 weeks of doxycycline treatment. In addition, 6 weeks of doxycycline treatment resulted in decreased myelin debris both in midgraft and the distal nerve. Gastrocnemius and tibialis anterior muscle mass were similar to that of the isograft group and significantly higher than all other groups. This study demonstrated that the

temporal and spatial control of GDNF release might play a major role in causing the "candy-store" effect. Normal doxycycline-inducible system in preclinical studies showed loss of transduced cells caused by an immune response to the foreign transactivator in rodents and non-human primates [133–137]. A recent study used an immune-evasive doxycycline-inducible gene switch to control GDNF expression in avulsed reimplanted ventral spinal roots [138]. GDNF expression was either constitutively on or turned on for 1 month. Both groups with GDNF expression were able to improve motor neuron survival. However, retrograde tracing from the sciatic nerve (10cm distal from the implantation site) showed a higher number of labeled motor neuron with 1 month of GDNF expression than all other groups, including constitutive GDNF expression. The number of fibers observed in the sciatic nerve was also the highest. Functional recovery, measured by compound muscle action potential of the gastrocnemius and plantar muscle, was better with the 1 month of GDNF expression 24 weeks post-repair. This study again showed that the controlled release of GDNF could significantly impact axon entrapment. As previously mentioned, the mechanism by which GDNF causes the "candy-store" effect is still unknown. Understanding this mechanism can help us develop GDNF delivery strategies that reduce axon entrapment.

1.5 Concluding Remarks

In this body of work, we aim to study the underlying mechanism by which GDNF causes the "candy-store" effect. All previous studies that demonstrated axon entrapment were *in vivo*. However, given the complexity of the *in vivo* environment and the involvement of multiple cell types in the PNS, it can be difficult to study and understand individual components and factors that cause axon entrapment. Here we want to develop an *in vitro* culture platform using a microfluidic device that enables clear visualizations of axon extensions under various conditions that could cause axon entrapment. In addition, we wish to explore how GDNF impact SCs and

neuron individually. By understanding the underlying mechanisms of how GDNF causes axon entrapment, we can better develop drug delivery methods that harness only the beneficial effects of GDNF while reducing the negative impacts.

Chapter 2: A microfluidic platform to study the effects of GDNF on neuronal axon entrapment

2.1 Abstract

One potential treatment strategy to enhance axon regeneration is transplanting Schwann Cells (SCs) that overexpress glial cell line-derived neurotrophic factor (GDNF). Unfortunately, constitutive GDNF overexpression *in vivo* can result in failure of regenerating axons to extend beyond the GDNF source, a phenomenon termed the "candy-store" effect. Little is known about the mechanism of this axon entrapment *in vivo*. We present a reproducible *in vitro* culture platform using a microfluidic device to model axon entrapment and investigate mechanisms by which GDNF causes axon entrapment. The device is comprised of three culture chambers connected by two sets of microchannels, which prevent cell soma from moving between chambers but allow neurites to grow between chambers. Neurons from dorsal root ganglia were seeded in one end chamber while the effect of different conditions in the other two chambers was used to study neurite entrapment. The results showed that GDNF-overexpressing SCs (G-SCs) can induce axon entrapment *in vitro*. We also found that while physiological levels of GDNF (100 ng/mL) promoted neurite extension, supra-physiological levels of GDNF (700 ng/mL) induced axon entrapment. All previous work related to the "candy-store" effect were done *in vivo*. Here, we

report the first *in vitro* platform that can recapitulate the axonal entrapment and investigate the mechanism of the phenomenon. This platform facilitates investigation of the "candy-store" effect and shows the effects of high GDNF concentrations on neurite outgrowth.

2.2 Introduction

Severe peripheral nerve injury (PNI) can have a devastating impact on patients' quality of life resulting in lifelong disabilities. Autologous nerve grafting has been the standard of care for PNI, despite its major disadvantage of donor site morbidity[18]. Alternative methods, such as acellular nerve grafts, are ineffective for large gaps because of the lack of cells and regenerative factors within the graft[139]. Even with proper surgical reconstruction, functional recovery can be incomplete[140]. Although the peripheral nerve is capable of regeneration, the rate of axonal regeneration is slow at 1-2 mm/day[2]. Patients suffering from proximal injuries, such as brachial plexus injuries, which can involve regeneration distances of up to a meter, may require 2-3 years for axons to reach target muscles[18]. However, chronic denervation can result in quiescence of Schwann cells (SCs), which leads to their precipitous decline in growth factor expression and a progressive failure to promote axonal regeneration over time[139]. In addition, essentially irreversible changes to muscle occur by 12-18 months[141], at which point functional recovery is unlikely. To treat these patients, it is critical to devise strategies to enhance axonal growth and prevent chronic denervation of SCs to promote robust axon regeneration over long distances. One appealing strategy to improve recovery is to use exogenous growth factors and/or SCs with exogenous growth factor expression to enhance axonal regeneration.

Glial cell line-derived neurotrophic factor (GDNF) is one of these potent growth factors involved in the normal regenerative process after injury. GDNF has been shown to improve axonal regeneration in motor neurons[4] and a subset of sensory neurons[5]. *In vitro* studies have shown that

GDNF forms a complex with GDNF family receptor alpha 1 (GFRα1) and acts as an axonal guidance signal during regeneration[6,8,10,11]. Although SCs intrinsically secrete GDNF following injury, they are unable to maintain this trophic support for neurons over long periods of time after injury[30]. In rodents, injury-induced GDNF expression is insufficient to stimulate axonal regeneration after 2 months and decreases to baseline level by 6 months[30]. Therefore, one viable strategy to increase the regeneration window is to develop effective delivery systems for GDNF over a long period of time.

Various methods of delivery have been developed including protein delivery systems, gene therapy, and cell therapy. In particular, the use of adeno-associated and lenti-viral vectors that encode GDNF have been used in many studies. Our lab and others have previously studied lentiviral mediated overexpression of GDNF from SCs (GDNF-overexpression SCs, or G-SCs)[5,6,8,130]. However, excess GDNF production causes the "candy-store" effect, where axons do not extend beyond sources of GDNF expression and are entrapped at a site rich in growth factor[8,9,130] (Fig. 2.1). Axonal swirling and coils form at these GDNF sources and are composed of a large number of motor axons and densely packed SCs[9,130]. Inside the axon coils, myelination is severely impaired as shown by a decrease in myelin basic protein expression[130]. These negative side effects create a major barrier against using GDNF

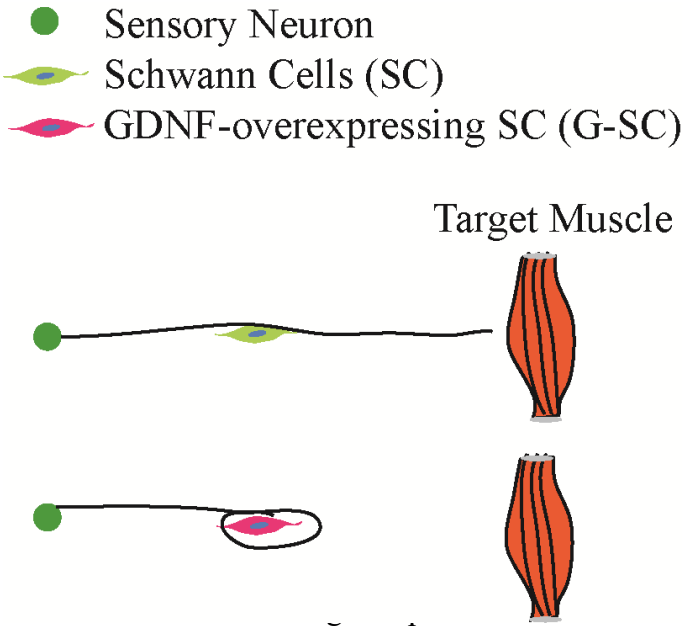

(SC) and reach towards target muscles (Top). When we constitutively overexpress GDNF in SCs (GDNF-SC), axons fail to extend beyond the GDNF source (Bottom), causing the Candy-store effect

to promote axonal regeneration. Understanding the "candy-store" effect is important for effectively using GDNF to promote axonal regeneration and reduce its negative impact. Studying the "candy-store" effect *in vivo* is challenging given the involvement of multiple cell types and the complex peripheral nerve environment. In contrast, *in vitro* investigation will enable us to conduct controlled studies of individual factors. However, standard *in vitro* culture platforms cannot spatially separate neurons from extending neurites for clear visualization. Alternatively, microfluidic devices have been extensively used to model nerve injury[126,142–145], with the major advantage of easy fabrication of the topographical structures of the culture platform. Namely, microfluidic devices can have features on the micrometer scale, which is ideal for isolating neurite extensions from neuronal soma. Therefore, developing a microfluidic device for recapitulating axon entrapment will allow for investigating the mechanism of the "candy-store" effect.

In this study, we developed a microfluidic device to recapitulate the "candy-store" effect *in vitro* and examined the effects of G-SCs on neuronal axon entrapment. Neurite extension was quantified in neuron-SCs (normal SCs) and neuron-G-SCs (GDNF overexpressing) co-cultures. We also investigated the effects of different GDNF concentrations on axon entrapment. G-SCs resulted in significantly greater trapping compared to normal SCs indicating that G-SCs can entrap neurites *in vitro*. In addition, high GDNF concentrations led to a similar decrease in neurite extension suggesting that high GDNF levels alone are sufficient to entrap axons.

2.3 Materials and Methods

2.3.1 Fabrication of Microfluidic Device Master Mold

3-inch silicon wafers (Silicon Inc. ID, USA) were coated with SU-8 5 photoresists (MicroChem Corp, MA, USA) using a spin-coater. The wafers were then exposed under UV light under (or through) the first layer of photo mask that had the pattern for the microchannels (Fig. 2.2). After development, the wafers were coated with a layer of SU-8 2050 and exposed under the second photo mask, which contained the pattern for the cell culture chambers. After development, the wafers were exposed to trichloro(1,1,2,2-perfluorooctyl) silane (Millipore Sigma, MO, USA) under vacuum for 1 hour to form an antiadhesive layer.

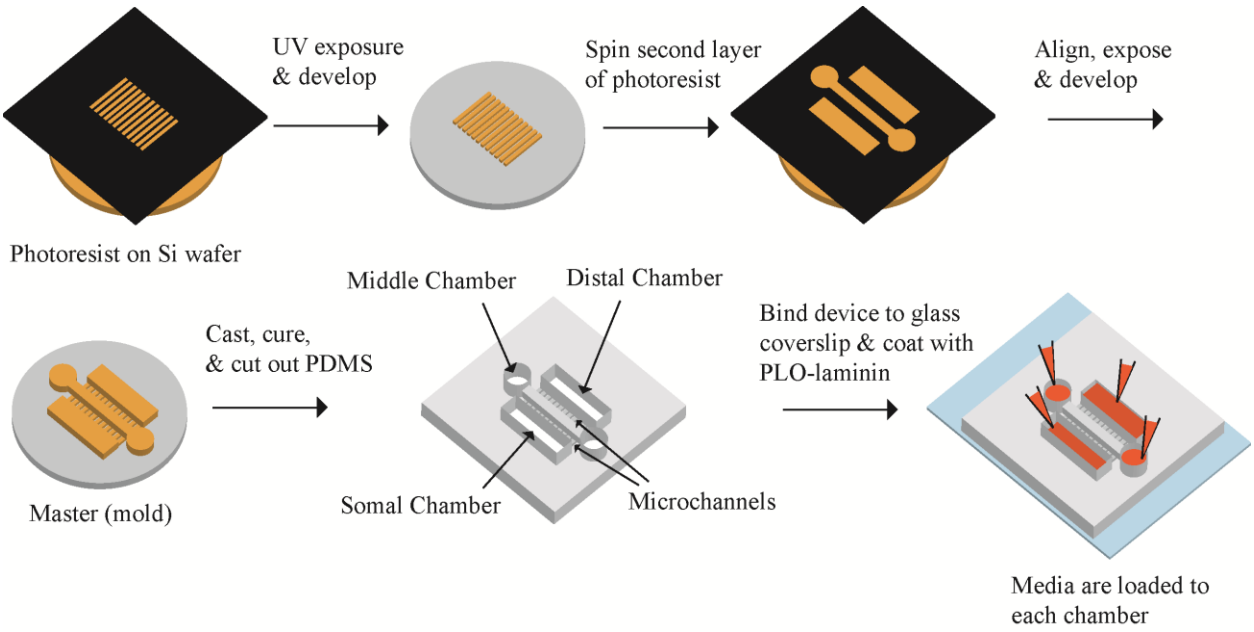

Figure 2.2: Schematics of Microfludic Device Fabrication Process. The master mold for the device consist of two layers of photoresist structures. The first layer defines the microchannels at 5 µm height. The second layer defines the culture chambers at 100 µm height. Soft lithography is used to make PDMS device, which is then assembled with glass coverslip as bottom and coated with PLO-laminin. The three chambers are connected by two sets of microchannels. The middle chamber is accessed through the two circular reservoirs.

2.3.2 Soft Lithography and Microfluidic Device

Polydimethylsiloxane (PDMS, Sylgard 184, Dow Corning, MI, USA) was poured onto the silicon master mold in a petri dish with 1:10 weight ratio of curing agent to base and put under vacuum to remove air bubbles (Fig. 2.2). The PDMS was cured at 60°C overnight. The device was then cut out and bonded to a glass slide using a plasma cleaner (Plasma Clean PDC-001, Harrick Plasma Inc., NY, USA). After 20 minutes of UV sterilization, the completed device was coated with 0.01% poly-L-ornithine (PLO) for 1 hour at 37°C and laminin (1 mg/mL, Life Technologies, CA. USA) for 1 hour at 37°C.

2.3.3 FITC Conjugation and Protein Transport Quantifications

Fluorescein isothiocyanate (FITC) conjugation was performed as directed by the manufacturer (Sigma). Porcine pepsin (35 kD, Sigma) was used as an alternative to GDNF (30.4 kD) for protein labeling because of their similar sizes. After completion of the conjugation, the FITC-labeled protein was in PBS solution with 1% bovine serum albumin (Sigma). Various volumes of FITC-labeled protein (1 µg/mL) in solution were then applied to the distal chamber with the expectation that higher volumes would increase protein transport to the somal chamber. After 24 hrs, the liquid from the somal chamber was collected and the fluorescence was measured at 488nm using a fluorescence spectrophotometer (SpectraMax M2e, Molecular Devices, CA, USA). The percent fluorescence was calculated as a percentage of somal chamber fluorescence intensity over distal chamber fluorescence intensity.

2.3.4 Isolation of Sensory Neurons and Culture Conditions

Sensory neurons were harvested from White Leghorn chicken (Texas A&M University, Texas, USA) embryos at Day 7-9. Dorsal root ganglia were isolated from embryos and dissociated using 0.25% trypsin-EDTA (Invitrogen, CA, USA) for 20 minutes at 37°C. Dissociated neurons were seeded in the somal chamber at 85,000 cells/cm2 and cultured in neurobasal medium with 2% B27 supplement, 1% penicillin-streptomycin (Pen/Strep), and 1% GlutaMAX (Invitrogen) (Fig. 2.3). Glial cell-line derived neurotrophic factor (GDNF, PeproTech, NJ, USA) was applied to the middle and/or distal chamber. Medium in the somal chamber was replaced with fresh medium every two days. Medium in the middle and distal chamber was also replaced every two days to maintain the GDNF level. By replacing media every two days in all chambers, the volumes of each chamber was maintained.

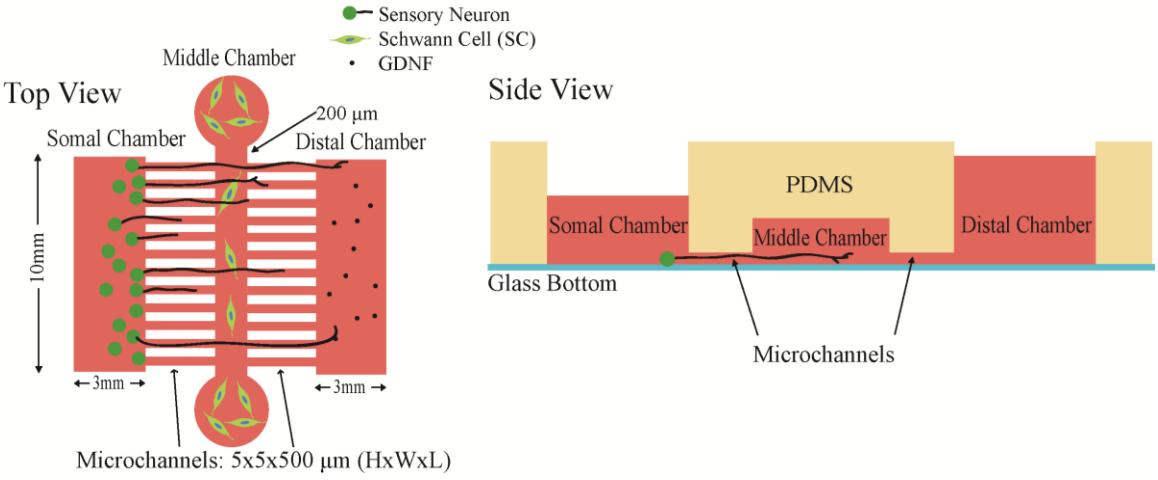

Figure 2.3: Schematics of the microfluidic device. A) Top and B) side views of the microfluidic device. Both Somal and Distal chambers have a surface of 10 mm×3 mm (schematics are not drawn to scale). Middle chamber reservoirs are 5mm in diameter and the chamber dimensions are 100 mm × 200 µm × 100 µm (L×W×H). The two sets of microchannels dimensions are 5 × 5 × 500 (L×W×H) µm. Side view shows different volumes applied to each chamber. The volume applied to the middle chamber is the volume applied to the two circular reservoirs.

2.3.5 Schwann Cell Harvest and Culture

SCs were harvested from sciatic nerves collected from adult male Lewis rats using previously described methods[146]. To isolate the SCs, first nerve branches were placed in DMEM (Dulbecco's Modified Eagle Medium) with sodium pyruvate (110 mg/L, Invitrogen), Collagenase (10 mg/mL, Thermo Fisher), and 0.25% trypsin for 30 min at 37 °C. After triturating the branches, they were centrifuged for 10 min at 500×*g*, and the cell pellet was washed with SC medium containing DMEM plus 10% fetal bovine serum (FBS, Life Technologies) and 1% Pen/Strep. The cells were then plated into a 100 mm petri dish coated with 0.1% poly-L-lysine (Sigma) and laminin. Cytarabine (Ara-C, 10 μM, Sigma) was added to the plate along with fresh SC medium on Day 3 after plating. Then the plate was supplemented with 2 μM forskolin (BioGems, CA, USA) with fresh SC medium and cultured for 1-2 weeks before use. G-SCs were generated based on a protocol previously developed [5]. Briefly, SC cultures were transduced with lentiviral particles containing GDNF transfer plasmid before passage 7. Cells were incubated with 2 μg/mL of polybrene (Santa Cruz Biotechnology, TX, USA) in SC medium for 1 hour at 37°C, after which the lentiviral vectors containing GDNF are introduced (MOI = 35). Cells are then incubated with 2 μg/mL polybrene and vector for 20 hours at 37°C. G-SCs were tested using enzyme-linked immune-sorbent assay (ELISA, R&D Systems, MN, USA) for GDNF production according to previously published results [5]. G-SCs were seeded in the middle chamber at 100,000 cells/cm^2. G-SCs produced 106.2±6.8 ng/mL/day of GDNF in the middle chamber. Based on this GDNF production, approximately 744 ng/mL of GDNF was produced over 7 days. Therefore, we used 700 ng/mL of GDNF as the supra-physiological level to be applied in the middle chamber.

2.3.6 Immunocytochemistry and Data Quantification

Immunocytochemistry (ICC) was performed on Day 6 after the start of neuronal culture. Briefly, the cells in the device were fixed using 4% paraformaldehyde (Sigma) for 20 min. After washing 3 times with PBS, the cells were permeabilized with 0.01% Triton X-100 (Sigma) for 20 min. The cells in the device were then blocked using 5% normal goat serum (NGS, Sigma) in PBS for 1 hr. Primary antibodies used included anti-neurofilament (1:200 with 2% NGS in PBS, clone 3A10, Developmental Studies Hybridoma Bank, IA, USA) for neurites and anti-S100β (1:400 with 2% NGS in PBS, Polyclonal Rabbit Ant-S100, Dako, CA, USA) for SCs. After incubating with primary antibodies overnight, the device was washed 3 times with PBS and then secondary antibodies were applied for 2 hrs. Hoechst 33342 was applied (1:1000 dilution) for 20 min after washing the device with PBS. The device was then imaged using a wide-field fluorescence microscope (Leica DMi8, Leica, IL, USA). After acquiring images of the middle chamber and microchannels, neurites were quantified as a percentage of axons crossing, namely, the number of neurites exiting the middle chamber was divided by the number of neurites entering the middle chamber (Fig. 2.5). Overlapping neurites in one microchannel are accounted for by tracing them for a short distance after exiting the microchannel, at which point the neurites disperse (typically 3-4 neurites, data not shown).

2.3.7 Statistical Analysis

One-way ANOVA is performed on the sample groups using Minitab software. Scheffe's post-hoc test with $p<0.05$ for significance was used. Data represented were shown as mean ± standard deviation. Data included N = 8 or more devices per condition; n=30-518 neurites measured per device.

2.4 Results

2.4.1 Microfluidic device development

One of the key features in the design of this microfluidic device was that it should enable cell signaling through exogenous growth factors and/or cell-cell interactions. Therefore, it was important to test protein transport from distal chamber to somal chamber in the microfluidic device to ensure that factors in the distal chamber could elicit a response in neurons separated by microchannels. We also sought to determine whether a growth factor in the distal chamber could provide axon guidance and/or promote survival of neurons seeded in the other chamber. We used pepsin (35 kDa), a similarly sized protein to GDNF (30.4 kDa), conjugated with fluorescein isothiocyanate (FITC) to examine the transport of proteins between the distal and somal chamber. FITC-pepsin was applied to the distal chamber and the fluorescence intensity in the somal chamber was measured over time. This allowed an estimation for the amount of GDNF that will reach the somal chamber for neurons to detect, and thus was used to determine the initial GDNF concentration that should be applied to the distal chamber to obtain a physiologically relevant level in the somal chamber.

We tested whether protein transport can be controlled by modulating the volume in each chamber (and thus the pressure differential) such that fluid was only flowing unidirectionally from the distal to the somal chamber. Two different volume sets were applied to the device. The first set of conditions tested had 50 µL of liquid in the somal and the middle chamber, and 100 µL of liquid in the distal chamber (Fig. 2.4A, 50/50/100). After 24 hours, the fluorescence intensity in the somal chamber was 6.6±2.0% of the initial fluorescence intensity in the distal chamber. The second set of conditions had 110 µL of liquid in the middle chamber, and 170 µL in the distal

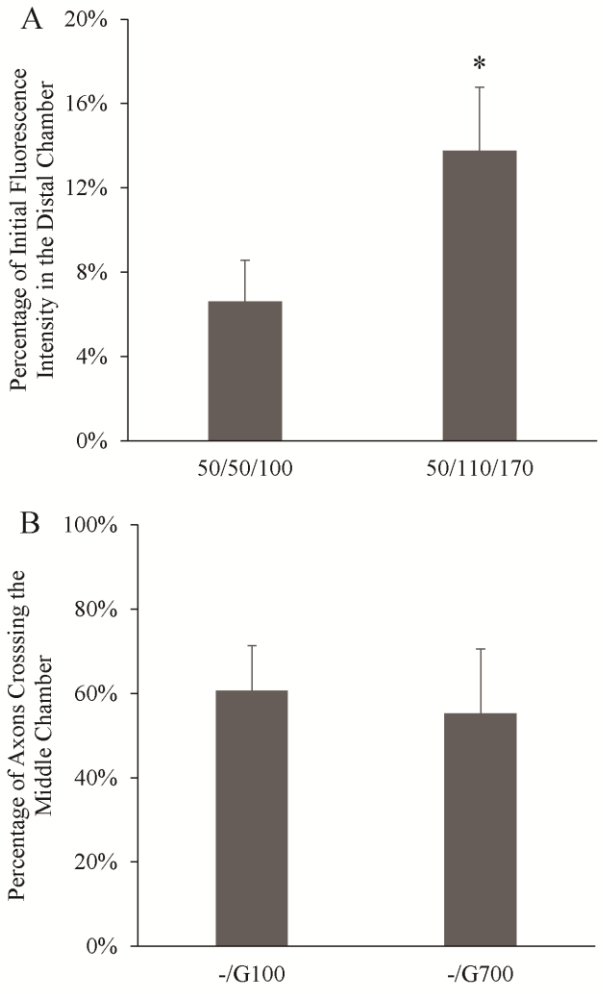

Figure 2.4: Microfluidic device shows controlled protein transport and robust axon crossing. A) Varying the loading volume in each chamber changes the amount of protein transported. 50/50/110 correspond to the volumes in somal/middle/distal chamber in μL. With a volume increase in the distal and middle chamber, the amount of fluorescence increased more than 2-fold (6.6% to 13.8%). *: $p<0.05$ N=4. B) Quantification of axons crossing the middle chamber with different conditions. Both conditions showed robust axons crossing (-/G100 at 64.6%±10.7%, -/G700 at 55.3%±15.2%). N = 8.

chamber. The fluorescence intensity increased to 13.8±3.0% (Fig. 2.4A, 50/110/170). This demonstrated that protein concentration in the somal chamber can be controlled by varying the volume applied to the other two chambers.

To test whether high GDNF concentrations can cause axon entrapment *in vitro,* we wanted to first establish a positive control that allows neurites to robustly cross the middle chamber. Table 2.1 shows the conditions applied to the middle and distal chambers. Either no GDNF, 100ng/mL, or 700ng/mL of GDNF was added to the respective chambers. No growth factor addition resulted in low neurite outgrowth into the middle chamber (<30 neurites/device). Even though the percentage of axon crossing was low under this condition, it did not represent the axonal entrapment effect but likely a result of poor neurite extension in the first place. We found that with 100 ng/mL and 700 ng/mL of GDNF in

the distal chamber and 0 ng/mL in the middle and somal chamber, neurites were able to robustly grow across the middle chamber to reach the second set of microchannels (Fig. 2.4B). Both conditions showed at least 50% of axons crossing with an average of 261 neurites measured in each device. These two conditions were used positive controls to compare with potential axon trapping conditions.

2.4.2 GDNF-overexpressing Schwann cells show axon entrapment in the microfluidic device

To mimic the *in vivo* axon entrapment in the microfluidic device, we evaluated the effects of placing G-SCs in the middle chamber, on neurite outgrowth compared to normal Schwan cells (Table 2.1). Briefly, we seeded DRG neurons in the somal chamber and normal SCs or G-SCs in the middle chamber (Fig. 2.5). We found that seeding normal SCs in the middle chamber resulted in robust axon growth resulting 59.2% axons crossing (Fig. 2.6C, SC/-), comparable to 100 ng/mL of GDNF in the distal chamber (Fig. 2.4B). In contrast, seeding G-SCs in the middle chamber significantly reduced the percentage of axons crossing to the distal chamber to 25.3% (Fig. 2.6C,

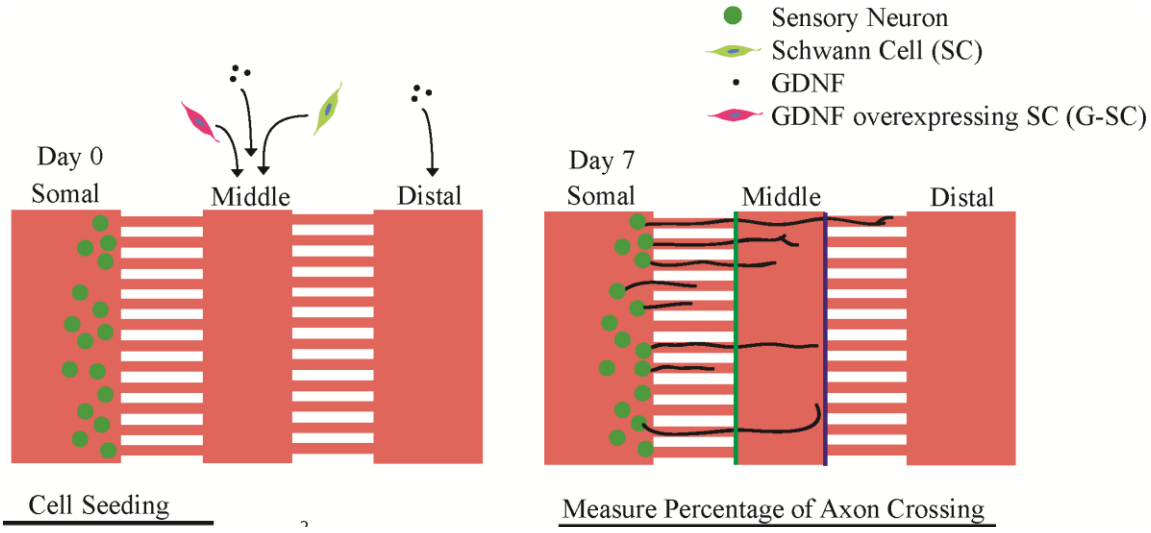

Figure 2.5: Schematics of culturing conditions. Neurons are seeded on Day 0 and stained on Day 7 using immunocytochemistry (ICC), at which point the percentage of axons crossing is quantified. Different Schwann cells or GDNF concentrations are applied to the middle chamber and distal chamber (Table 2.1).

G-SC/-). These results demonstrated that G-SCs can induce axon entrapment *in vitro*. It was also noted that neurites with G-SCs seeded in the middle chamber formed a dense network of fibers along the G-SCs (Fig. 2.6B), while neurites with normal SCs do not demonstrate this behavior (Fig. 2.6A). This resembled morphologies observed in previous *in vivo* studies where axons tend to form nerve coils at the sites of GDNF overexpression[8,130].

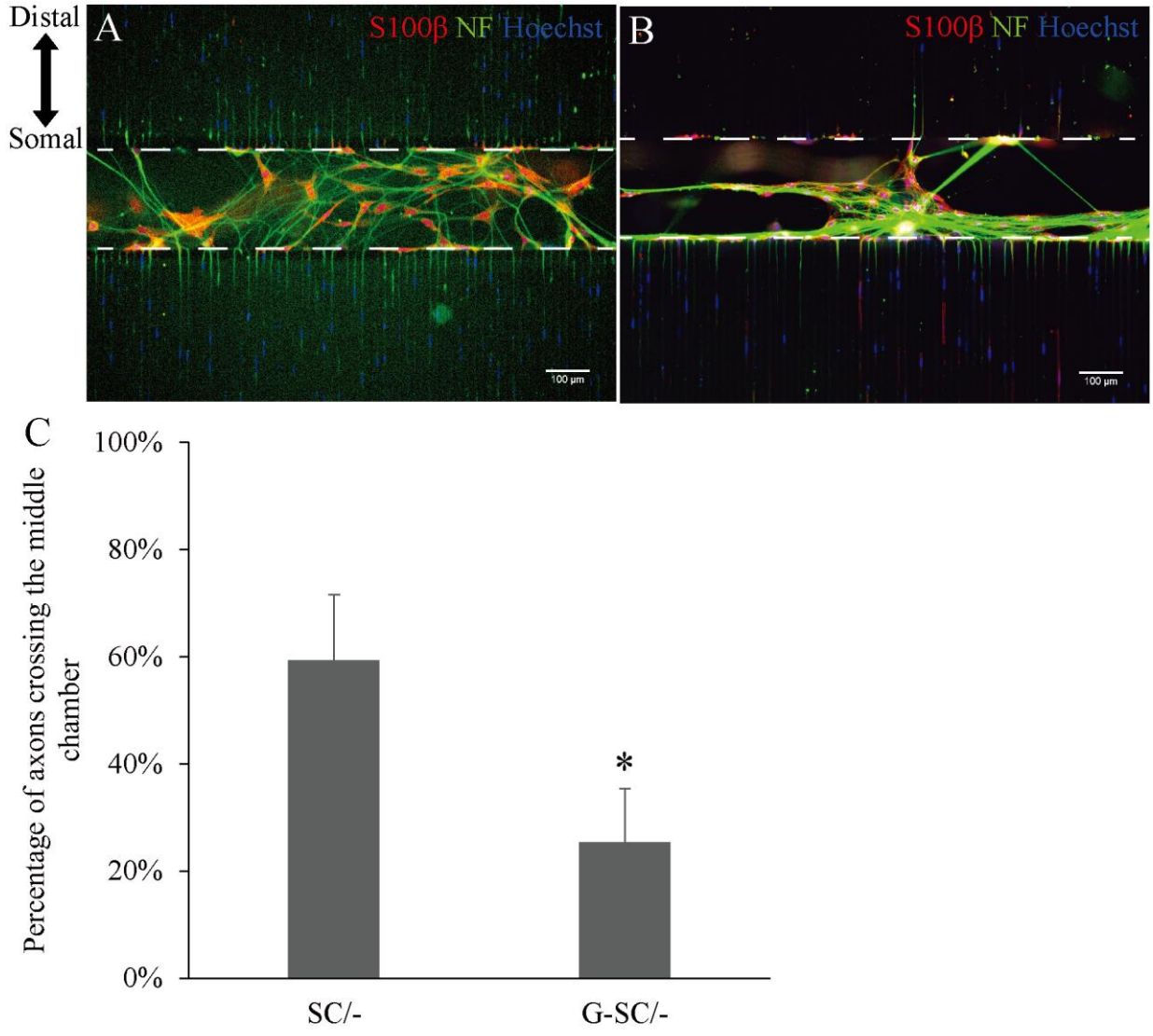

Figure 2.6: GDNF-Overexpressing Schwann Cells causes axonal trapping *in vitro*. A-B) Normal Schwann Cells (A) and G-SCs (B) seeded in the middle chamber. C) Quantification of axons crossing. SC results in 59.2±12.3%. G-SC results in 25.3±9.9%. N=8. *: $p<0.00005$

Table 2.1
List of conditions applied to the middle and distal chambers

MIDDLE CHAMBER	DISTAL CHAMBER		
SCHWANN CELLS	None		
GDNF-OVEREXPRESSING SCHWANN CELLS	None		
CONTROL (NO GDNF)	None	GDNF (100ng/mL)	GDNF (700ng/mL)
GDNF (100 NG/ML)	None	GDNF (100ng/mL)	GDNF (700ng/mL)
GDNF (700 NG/ML)	None	GDNF (100ng/mL)	GDNF (700ng/mL)

2.4.3 Effects of differential GDNF concentrations on neurite extensions

We wanted to examine the effects of different concentrations of GDNF in the middle and distal chambers (Table 2.1). Previous *in vitro* studies had shown that physiological levels of GDNF (100 ng/mL) improve neurite outgrowth[126]. In addition, applying 100 ng/mL of GDNF to the distal chamber also promoted robust neurite outgrowth towards the distal chamber. Based on the GDNF production from G-SCs, approximately 744 ng/mL of GDNF was produced over 7 days. Therefore, we used 700 ng/mL of GDNF as the supra-physiological level. GDNF uptake by neurons was qualitatively assessed by ICC staining of GDNF. Cell treated with 700ng/mL of GDNF showed greater levels of antibody staining compared to untreated cells and cell treated with 100ng/mL of GDNF (Fig. 2.7). We found that supra-physiological levels of GDNF in the middle chamber significantly reduced the percentage of axons crossing the middle chamber (Fig. 2.8G). Applying 100 ng/mL of GDNF to the middle chamber with 700 ng/mL in the distal chamber did not reduce the percentage of axons crossing comparing to 100 ng/mL in the distal chamber and 0 ng/mL in the middle chamber (Fig. 2.8G, -/G100, G100/-). However, 700 ng/mL of GDNF in the middle

chamber and 0 ng/mL in the distal chamber significantly reduced the percentage of axons crossing to 14.0% (Fig. 2.8D & G, G700/-). This suggests supra-physiological levels of GDNF can induce axon trapping *in vitro*. Immunostaining for neurofilament showed that neurites tend to stay in the middle chamber; however, we did not observe the formation of dense fibers networks observed with G-SCs. We also examined the effects of GDNF at 250 ng/mL and 500 ng/mL applied in the middle chamber and 0 ng/mL in the distal chamber (G250/-, G500/-). G250/- showed axons crossing at 40.6%±12.4%; while G500/- showed axons crossing at 45.8%±15.3%. This indicates the threshold concentration for GDNF to induce axon entrapment appears to be between 500 ng/mL and 700 ng/mL.

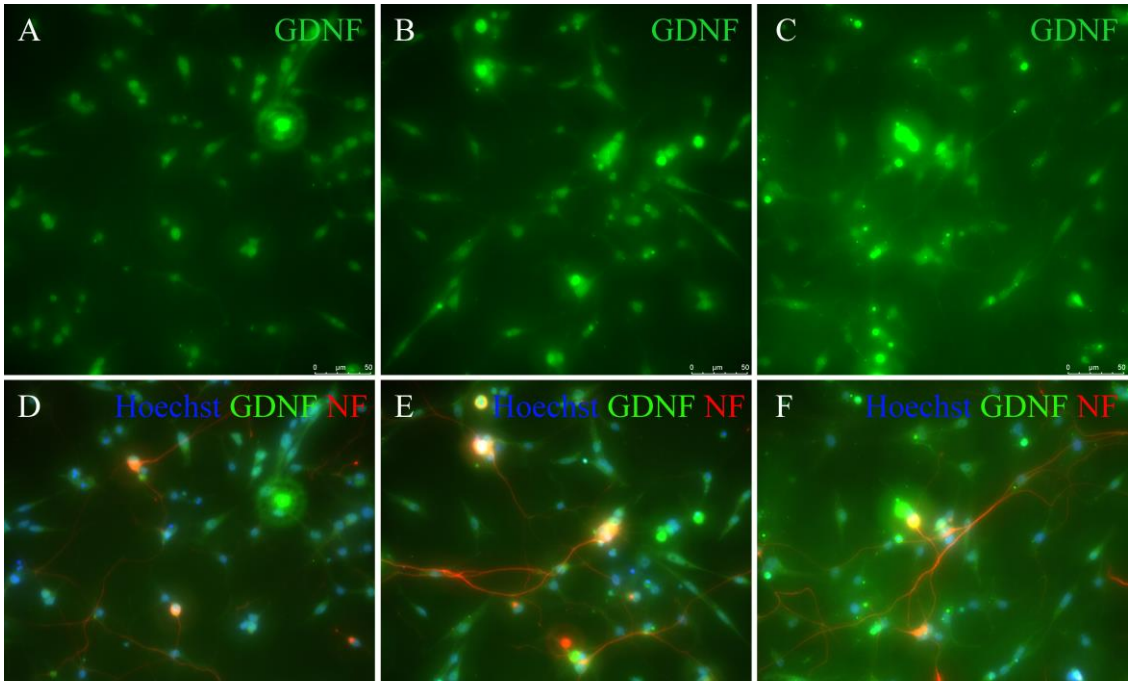

Figure 2.7: Immunocytochemistry of GDNF Uptake by the Dissociated DRGs. Dissociated DRGs are cultured in 48-well plates and immunostained with GDNF- and neurofilament-antibodies. A-B) Untreated and 100ng/mL of GDNF treated cell cultures showed relatively weak GDNF fluorescent signals. Untreated condition showed some signals likely because of the SCs present in the dissociate DRG cultures. SCs are known to secrete GDNF in cell culture [197]. C) Dissociated DRGs treated with 700ng/mL of GDNF showed stronger fluorescent signals compared to the other groups. D-F) Merged image of GDNF with Neurofilament and Hoechst nuclear stain.

Next, we wanted to see whether adding GDNF to the distal chamber can overcome the axon trapping induced by applying high levels GDNF to the middle chamber (Fig. 2.8H). When 100 ng/mL of GDNF was in both middle and distal chambers, 54.8% of axons were able to cross the middle chamber, similar the result observed with the same concentration of GDNF added to either just the distal or just the middle chamber (Fig. 2.8B, G100/G100). This suggests that axons were not trapped by a uniform distribution of GDNF at a physiological concentration. In contrast, applying supra-physiological levels of GDNF in the middle chamber and physiological GDNF levels to the distal chamber reduced the percentage of axons crossing to 24.3% (Fig. 2.8E & H, G700/G100). Therefore, physiological GDNF levels at a more distal site to the neurons cannot overcome axon trapping induced by high GDNF levels at a more proximal site. More importantly, when supra-physiological GDNF is applied to both the middle and distal chambers, only 14.1% of axons were able to cross the middle chamber (Fig. 2.8F & I, G700/G700), suggesting that high GDNF levels also cannot abolish axon trapping. Together, these data suggest that supra-physiological levels of GDNF have a direct effect on reducing neurite outgrowth.

2.5 Discussion

A number of studies have focused on the use of exogenous growth factors for treating peripheral nerve injuries. Growth factors, such as GDNF, are released by SCs in response to nerve injury and aid neuronal survival and axon regeneration[3]. Many studies have shown that GDNF also acts as a directional cue for guidance of regenerating axons [147,148]. In addition to its direct benefits, GDNF also contributes to the ability of SCs to promote repair after injury. The presence of GDNF enhances the ability of SCs to myelinate axons by inducing differentiation of a myelinating phenotype[122–124]. As a result of their growth promoting benefits, various methods for the

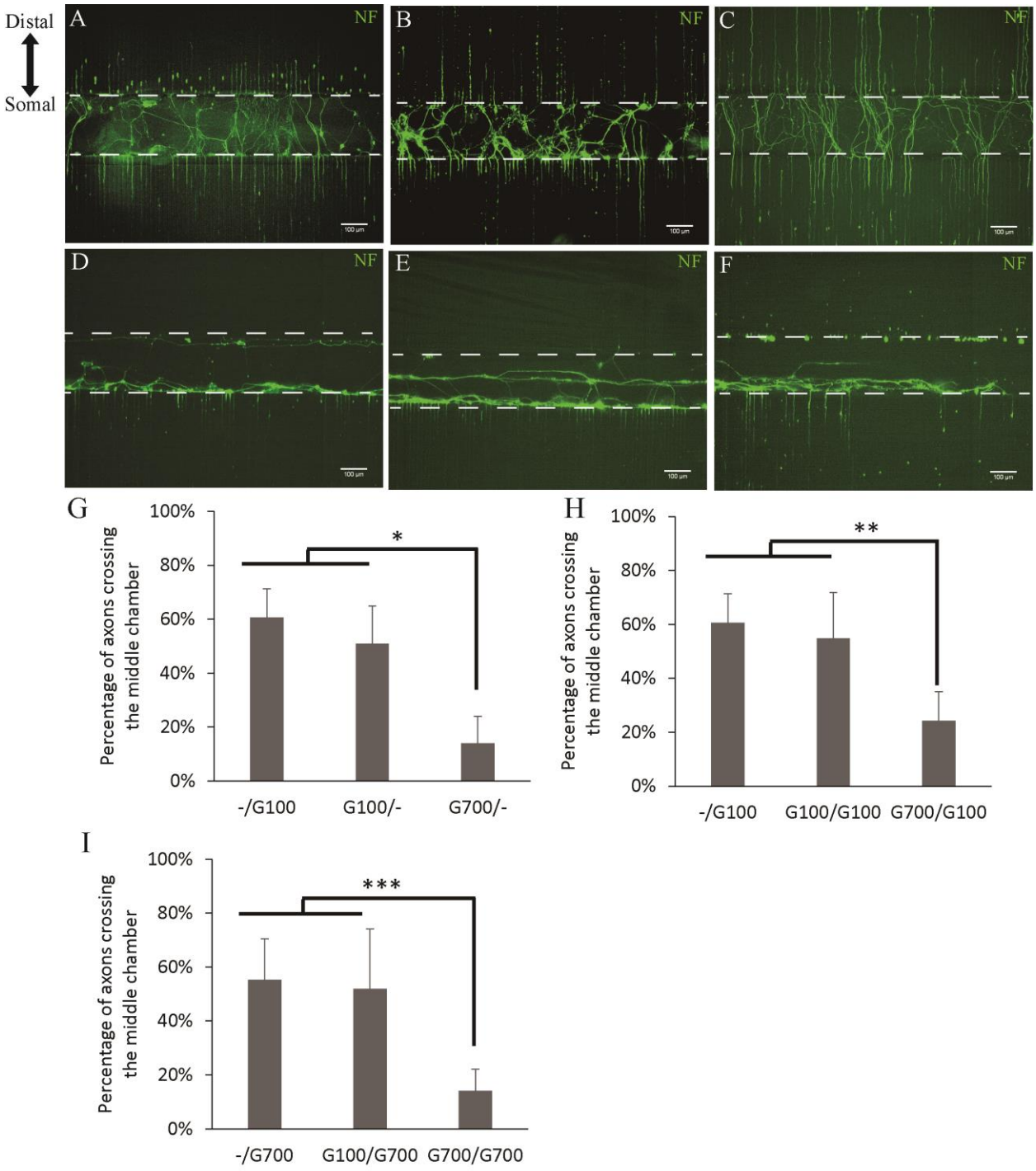

Figure 2.8: Effects of differential GDNF concentrations on neurite extensions. A-C) Low (100ng/mL) GDNF applied to the middle chamber with varying concentrations in the distal chamber. A) G100/- at 50.9±14.0%; B) G100/G100 at 54.8±17.0%; C) G100/G700 at 51.8±22.2%. D-F) High (700ng/mL) GDNF applied to the middle chamber with varying concentrations in the distal chamber. D) G700/- at 14.0±10.0%; E) G700/G100 at 24.3±10.7%; F) G700/G700 at 14.1±8.1%. G-I) Quantification of axons crossing with varying concentrations of GDNF applied to the middle chamber and distal chamber. N=8. *: $p<0.00005$, **: $p<0.05$, ***: $p<0.005$.

delivery of growth factors have been examined including using lentiviral[9,149] or adenoviral injections[150], microspheres[34,151], and scaffolds and conduits[152]. Yet, there still remains much to be understood about the effects of growth factors on axon regeneration.

Unlike other growth factors[153–155], GDNF when overexpressed can cause axon entrapment within the zone of GDNF expression, and is thus dubbed the "candy-store" effect[8,9,130,132,156]. This behavior was first shown by Blits *et al.*, where adenoviral-mediated overexpression of GDNF near the motoneuron pool promoted axon sprouting but prevented directional growth of axons at denervated motoneuron pool. We and others have also observed a similar phenomenon when overexpressing GDNF after sciatic nerve injury with either viral expression or transgenic expression in SCs[6,130]. In order to resolve this issue, Eggers *et al*. generated a GDNF gradient *in vivo* using lentiviral vectors and found that even the lowest concentration of GDNF still entrapped axons. We and others have used tetracycline-inducible systems to temporally control GDNF overexpression and identified a critical window of time at which GDNF overexpression should be shut off [6,132]. However, little is known about the mechanism of the "candy-store" effect and whether it acts directly on axons or indirectly via SCs. Evidence suggests SCs undergo phenotypic changes in the presence of high levels of GDNF that could affect axon growth[130]. A recent study also shows G-SCs affect fibroblasts, and this interaction results in significant ECM remodeling [156]. However, all these studies have been done using *in vivo* models. The complexity of the *in vivo* environment presents a major challenge to eliciting the exact mechanism that underlies the "candy-store" effect. Here we developed a microfluidic device that enables us to conduct controlled studies of individual factors and provide spatial separation of neurons from extending neurites for clear visualization. This *in vitro* culture platform can help us understand why GDNF overexpression leads to the "candy-store" effect.

Previous studies have shown that G-SCs cause axon entrapment when transplanted in acellular nerve graft in sciatic nerve injury models[6]. Similarly, our results show that G-SCs cause axon entrapment in the microfluidic device. This demonstrates that our *in vitro* platform is able to mimic the *in vivo* phenomenon. Previous studies have shown that GDNF overexpression causes SCs to undergo phenotypic changes marked by a decrease in myelin basic protein and an increase in p75 receptor expression[130]. In this study, we observed that neurites form dense fiber networks along G-SCs, whereas these dense fibers were not observed in the presence of normal SCs (Fig. 2.6A & B). This dense accumulation of axons is strikingly similar to previous *in vivo* results where elevated GDNF expression from virally-induced cells resulted in thick fiber coils formed at GDNF overexpressing locations[8,130,156]. Our recent study showed that GDNF overexpression during nerve regeneration *in vivo* caused extensive axonal sprouting [156]. The evidence from these studies and our current studies suggests G-SCs play a major role in causing axon entrapment. Specifically, these cells can prevent neurites from extending beyond the region of elevated GDNF and induce the formation of fiber networks. GDNF gradients can guide axon regeneration from lower concentrations to higher concentrations and eventually lead to muscle cells as the final target in the PNS. It has been shown that viral vector-induced GDNF expression in myoblasts improved motor neuron survival [157]. Making myoblast as a source of neurotrophic factor would be particularly useful when nerves were close enough to the muscles to create a gradient that the axons could sense. Therefore, it might also be valuable to explore using myoblast as the source of neurotrophic factor for future studies of regeneration near the muscle.

In addition to investigating G-SC's effects on axon entrapment, we examined how exogenous GDNF affects neurite outgrowth in a microfluidic device. Previous studies have shown that GDNF applied at physiological levels (50 to 100 ng/mL) promoted axon growth [123,126]. In this

study, our results indicated that GDNF applied at a supra-physiological level (700 ng/ml) decreased neurite outgrowth. This suggests that a high GDNF level may be sufficient to trap axons. It is interesting to note that high GDNF levels in the distal chamber did not make up for axon entrapment caused by high GDNF in the middle chamber, suggesting axon entrapment is activated when GDNF reaches a certain threshold concentration and cannot be overcome by similarly high levels downstream. We also observed that neurites treated with high GDNF protein levels did not show dense fiber network formation. Compared to trapping caused by G-SCs, this might suggest the important roles of G-SC and ECM remodeling in axon entrapment and that the "candy-store" effect constitutes two parts, where axon trapping is caused by GDNF directly while fiber networks form after ECM remodeling and may involve SCs.

Understanding both the benefits and negative impacts of using growth factors is critical developing safe therapeutics. Here, we have developed a microfluidic platform that allowed us to investigate a major negative side effect of overexpressing GDNF from SCs. We have shown that G-SCs can induce axon entrapment similar to what is seen *in vivo*. In addition, this system allowed us to examine the effect of exogenous GDNF on neurite outgrowth. We have shown that high levels of GDNF alone can significantly reduce neurite outgrowth due to entrapment. Overall, this platform may provide a valuable tool to further investigate the underlying molecular mechanisms of the "candy-store" effect. Together, these findings may prove valuable as they provide directions toward devising drug delivery methods that harness only the beneficial effects of GDNF to establish a robust treatment system for PNI in animal models. Clinically, this project has the potential to lead to therapies that prolong the regeneration window for long gap PNI.

Chapter 3 Slitrk4 Activation by High GDNF Levels Leads to Neuronal Axon Entrapment

3.1 Abstract

Glial cell line-derived neurotrophic factor (GDNF) is a potent growth factor that affects both axon growth and the ability of Schwann cells (SC) to promote regeneration. Previous studies have shown that GDNF release through lentiviral-mediated overexpression can result in a "candy-store" effect, where the regenerating axons are entrapped and fail to extend beyond regions of high transgenic GDNF. We previously developed an *in vitro* culture platform that enables us to model the "candy-store" effect *in vitro*. In the current study, we used this platform to continue investigating the effect of GDNF on SCs' ability to promote axon regeneration and the underlying mechanisms of how GDNF can promote axon entrapment. We found that GDNF-overexpressing SCs (G-SCs) induced axon entrapment that cannot be overcome by high GDNF levels distally. SCs pre-conditioned with high GDNF concentrations also can cause axon entrapment; however, such pre-conditioned SCs cannot trap axons when high GDNF were present distally. After analyzing neuron gene expression changes after high levels of GDNF treatment, we found that SLIT and NTRK-like family member 4 (*SLITRK4*) was upregulated. Our results indicate that by knocking down *SLITRK4* expression using shRNA, axon entrapment was significantly reduced. Furthermore, inhibition of SLITRK4 ligand, protein tyrosine phosphatase σ (PTPσ), with PTP IV Inhibitor, a small molecule inhibitor, also significantly reduced axon entrapment. Our findings may provide valuable insight for understanding the effects of GDNF on peripheral nerve regeneration and contribute to developing better treatment strategies that harness the beneficial effects of GDNF without entrapment.

3.2 Introduction

Peripheral nerve injury (PNI) can severely impact patients' quality of life. Proximal injuries with a large gap between the two nerve ends are less likely to recover, as regenerating axons need to travel long distances over an extended time to reconnect to the end-organ targets [1]. Some of the main contributing factors to poor functional recovery include motor neuron apoptosis with chronic denervation and the decline of the growth-promoting capacity of Schwann cells (SC) [158–161]. After injury, SCs are known to de-differentiate and activate (alternative differentiation) to become "repair phenotype" SCs [93]. This process involves the downregulation of myelin-associated genes, upregulation of trophic factors and surface proteins providing support for injured neurons and substrates for growth cones, the formation of regeneration tracks for axon guidance, and activation of cytokines and autophagy for myelin breakdown directly, and by macrophages [162]. Important trophic factors and cell-surface proteins that support survival and axon growth include glial cell line-derived neurotrophic factor (GDNF), brain-derived neurotrophic factor (BDNF), and artemin, neurotrophin receptor p75 (p75NTR) and N-cadherin [26,27,93,163–166] . In particular, GDNF has been extensively studied for its effects on promoting axon regeneration, improving motor neuron survival, and guiding proper axon reinnervation leading to enhanced motor output [30,117,148,167–169]. Equally important are the effects GDNF has on SCs after injury. GDNF is known to affect SC maturation, migration, and proliferation [121,123,124,170–172].

Although exogenous GDNF has been shown to improved motor neuron survival and axon regeneration, efficient protein delivery is required due to the short half-life and poor tissue penetration of neurotrophic factors [127,128,173]. Gene therapy through adeno-associated and lentiviral-mediated methods of neurotrophic factors delivery ensures the local availability for the entire regeneration period [6,9,129]. However, we and others have shown that uncontrolled

overexpression of GDNF causes a "candy-store" effect, where axons do not extend beyond sources of GDNF expression and are entrapped at a site with high levels of GDNF overexpression [6,8,9,130,174]. Either by directly injecting lentiviral vectors for GDNF overexpression or transplanting SCs that overexpress GDNF at the injury site, large numbers of motor axons and SCs packed in coiled formations are observed at the GDNF expression site [6,9,130,132]. The negative side effects create a major barrier against using GDNF to promote axonal regeneration.

In a previous study, we developed a microfluidic device to recapitulate the "candy-store" effect *in vitro* and examined the effects of GDNF overexpressing SCs (G-SCs) on neuronal axon entrapment [174]. Similar to *in vivo* results, we found that G-SCs promote significantly greater axon trapping compared to normal SCs, indicating that G-SCs can entrap neurites *in vitro*. In the present study, we investigated the effects of pre-conditioning SCs with high GDNF levels and found that such treatment can also cause axon entrapment. In addition, we showed that axon entrapment caused by G-SCs could not be overcome by distal source of high GDNF levels (G-SCs), whereas entrapment caused by pre-conditioned SCs can be overcome by high GDNF. Previously, we also showed that soluble GDNF alone is sufficient to cause axon entrapment. To harness the growth-promoting effect and reduce the negative impacts of GDNF, it is important to understand the mechanism by which GDNF overexpression causes entrapment. To this end, we examined genes that are differentially expressed after exposing neurons to high GDNF levels and investigated potential gene targets that might contribute to axon entrapment using lentiviral-mediated mRNA knockdown. We identified that SLIT and NTRK like family member 4 (SLITRK4) was highly expressed in neurons treated with high levels of GDNF and that shRNA knockdown of SLIKTR4 in neurons significantly decreased neurite entrapment *in vitro*.

3.3 Materials and Methods

3.3.1 Microfluidic Device Fabrication:

Master molds were fabricated as described previously [175]. Briefly, 3-inch silicon wafers (Silicon Inc. ID, USA) were coated with SU-8 2 photoresist (MicroChem Corp, MA, USA) using a spin-coater. Exposing the photoresist under UV covered by the photomask forms the pattern for the microchannels. A layer of SU-8 2050 was then used to form the pattern for the cell culture chambers. Polydimethylsiloxane (PDMS, Sylgard 184, Dow Corning, MI, USA) was poured onto the silicon master mold in a petri dish with a 1:10 weight ratio of curing agent to the base and put under vacuum to remove air bubbles. The PDMS was cured at 60°C overnight. The device was then cut out and bonded to a glass slide using a plasma cleaner (Plasma Clean PDC-001, Harrick Plasma Inc., NY, USA). After 20 minutes of UV sterilization, the completed device was coated with 0.01% poly-L-ornithine (PLO) for 1 hour at 37°C and laminin (1 mg/mL, Life Technologies, CA. USA) for 1 hour at 37°C.

3.3.2 Isolation of Sensory Neurons and Culture Conditions:

Sensory neurons were harvested from White Leghorn chicken embryos (Texas A&M University, Texas, USA) at embryonic day 7-9. Dorsal root ganglia were isolated from embryos and dissociated using 0.25% trypsin-EDTA (Invitrogen, CA, USA) for 20 minutes at 37°C. Dissociated neurons were seeded in the somal chamber at 85,000 cells/cm^2 and cultured in neurobasal medium with 2% B27 supplement, 1% penicillin-streptomycin (Pen/Strep), and 1% GlutaMAX (Invitrogen) (Fig. 3.1). Glial cell-line derived neurotrophic factor (GDNF, PeproTech, NJ, USA) was applied to the middle and/or distal chamber. Medium in the somal chamber was replaced with fresh medium every two days. Medium in the middle and distal chamber was also replaced every two days to maintain the GDNF level. By replacing media every two days in all

chambers, the volumes of each chamber were maintained. PTP IV inhibitor (Santa Cruz Biotechnology, TX, USA) was dissolved in DMSO and applied at IC_{50}= 20μM according to manufacturer's recommendation. U73122 (Santa Cruz Biotechnology) was also dissolved in DMSO and was applied at a concentration of 5μM. Trapping control for the inhibitor study also has equal volumes of DMSO added.

3.3.3 Schwann Cell Harvest and Culture:

SCs were harvested from sciatic nerves collected from adult male Lewis rats using previously described methods [146]. To isolate the SCs, the sciatic nerve branches were placed in DMEM (Dulbecco's Modified Eagle Medium) with sodium pyruvate (110 mg/L, Invitrogen), Collagenase (10 mg/mL, Thermo Fisher), and 0.25% trypsin for 30 min at 37 °C. After triturating the branches, they were centrifuged for 10 min at 500×*g*, and the cell pellet was washed with SC medium containing DMEM plus 10% fetal bovine serum (FBS, Life Technologies) and 1% Pen/Strep. The cells were then plated into a 100 mm petri dish coated with 0.1% poly-L-lysine (Sigma) and laminin. Cytarabine (Ara-C, 10 μM, Sigma) was added to the plate along with fresh SC medium on Day 3 after plating. Then the cells were cultured in fresh SC medium supplemented with 2 μM forskolin (BioGems, CA, USA) and cultured for 1-2 weeks before use.

3.3.4 Lentiviral Transduction of Dissociated DRGs and SCs:

Dissociated chick DRG neurons were seeded overnight before the virus was applied. Lentiviral-shRNA particles were obtained from GeneTarget Inc (San Diego, CA). SLITRK4 (Sense strand: ACTATGCAAACTGCAGCTAAG) was silenced. A non-viral positive control condition treated with 700 ng/mL of GDNF and negative control with scrambled shRNA and GDNF treatment were used for comparison. The virus at MOI = 2.5 was applied to the cells. The plates were then centrifuged at 300g for 5 min. The cells were left with virus overnight in the

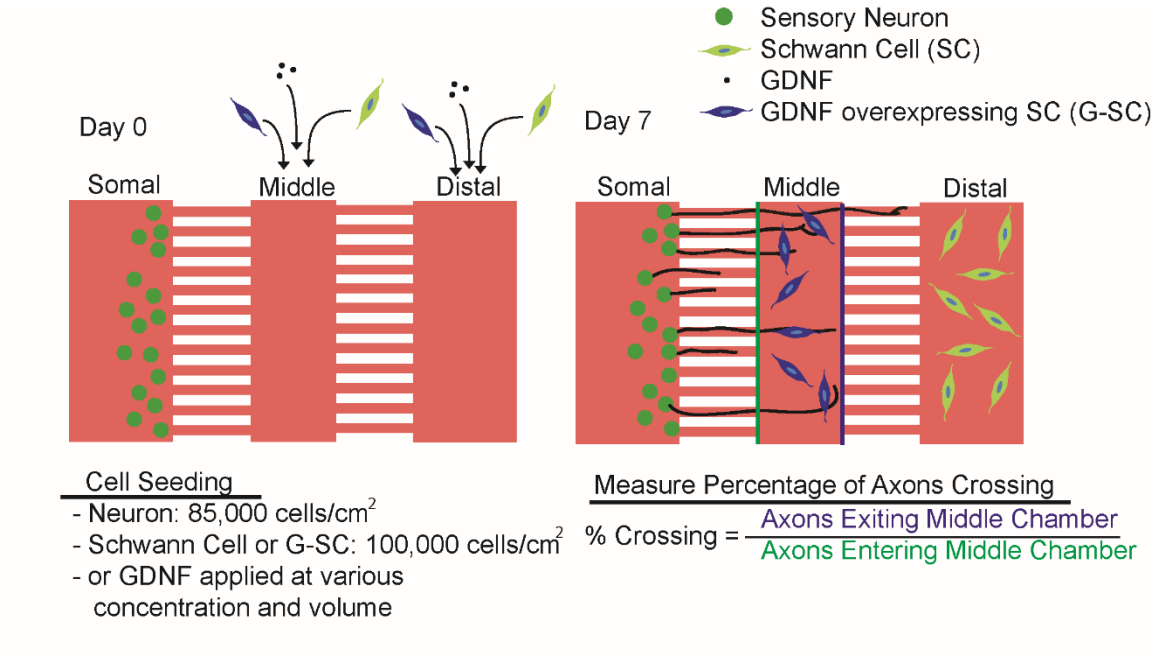

Figure 3.1: Diagram of experimental set up for neuron and SC co-cultures. Cartoon depiction of 3-chamber microfluidic devices seeded with dissociated DRGs in the somal chamber, and normal SCs or GDNF overexpressing SCs (G-SCs) in the middle or distal chamber. The microfluidic devices are composed of 3 chambers connected through 2 sets of microchannels with dimensions 5x5x500µm (LxWxH).

incubator. They were washed twice with neurobasal media and then cultured in neurobasal media plus supplement with GDNF. The cells were cultured for 7 days before they were evaluated for growth or collected for protein harvest. G-SCs were generated based on a protocol previously developed [5,7]. Briefly, full-length rat GDNF cDNA was cloned into a lentiviral expression vector in which gene expression was driven by the ubiquitin promoter and coexpression of DsRed fluorescent protein was enabled by an internal ribosomal entry site (IRES) element. The lentiviruses expressing GDNF were produced in HEK 293T cells (Li Lab, Washington University in St.Louis). SC cultures were transduced with lentiviral particles containing GDNF overexpression vectors before passage 7. Cells were incubated with 2 µg/mL of polybrene (Santa Cruz Biotechnology, TX, USA) in SC medium for 1 hour at 37°C, after which the lentiviral vectors

containing GDNF were introduced (MOI = 35). Cells were then incubated with 2 μg/mL polybrene and vector for 20 hours at 37°C. GDNF production level from the G-SCs was evaluated using enzyme-linked immune-sorbent assay (ELISA, R&D Systems, MN, USA) according to previously published results [5]. G-SCs were seeded in the middle chamber at 100,000 cells/cm^2. G-SCs produced 106.2±6.8 ng/mL/day of GDNF in the middle chamber. Based on this GDNF production, approximately 744 ng/mL of GDNF was produced over 7 days. Therefore, we used 700 ng/mL of GDNF as the supra-physiological level to be applied in the middle chamber.

3.3.5 Immunocytochemistry and Data Quantification:

Immunocytochemistry (ICC) was performed on Day 6 after the start of neuronal culture. Briefly, the cells in the device were fixed using 4% paraformaldehyde (Sigma) for 20 min. After washing 3 times with PBS, the cells were permeabilized with 0.01% Triton X-100 (Sigma) for 20 min. The cells in the device were then blocked using 5% normal goat serum (NGS, Sigma) in PBS for 1 hr. Primary antibodies used included anti-neurofilament (1:200 with 2% NGS in PBS, clone 3A10, Developmental Studies Hybridoma Bank, IA, USA) for neurons and anti-S100β (1:400 with 2% NGS in PBS, Polyclonal Rabbit Ant-S100, Dako, CA, USA) for SCs. After incubating with primary antibodies overnight, the device was washed 3 times with PBS, and then secondary antibodies were applied for 2 hrs. Hoechst 33342 was applied (1:1000 dilution) for 20 min after washing the device with PBS, to visualize nuclei. The device was then imaged using a wide-field fluorescence microscope (Leica DMi8, Leica, IL, USA). After acquiring images of the middle chamber and microchannels, percentages of axons crossing were calculated based on the number of neurites exiting the middle chamber divided by the number of neurites entering the middle chamber (Fig. 3.1). Overlapping neurites in one microchannel were accounted for by tracing them

for a short distance after exiting the microchannel, at which point the neurites disperse (typically 3-4 neurites, data not shown).

3.3.6 Gene Expression Analysis:

We used a DNA microarray to identify genes that were differentially expressed after high GDNF treatment. Dissociated embryonic chicken DRG's were treated with 0 or 700 ng/mL of GDNF for 7 days with media changes every two days. RNA was harvested using the RNeasy kit (QIAGEN, Valencia, CA). DNA microarray analysis was performed by the Genomics and Microarray Core at the University of Texas Southwestern using Affymetrix Chicken 1.0 ST array (Thermo Fisher). Data analysis was performed using the Transcriptome Analysis Console provided by Thermo Fisher. Data were normalized using the robust multiarray average. Statistical significance was evaluated using T-test with empirical Bayes statistics with $p < 0.05$ for a fold change of > |2|. False discovery rate was analyzed using the Benjamini-Hochberg procedure. Microarray analysis of G-SCs was published elsewhere [156].

We then used quantitative real-time PCR (qRT-PCR) to confirm the differential expression of selected genes. After harvesting RNA from dissociated DRGs, cDNA was made using the High Capacity RNA-to-cDNA Kit (Life Technologies, Carlsbad, CA). TaqMan Fast Advanced Master Mix (Life Technologies) was combined with TaqMan Gene Expression Assays (Life Technologies; Table X) and cDNA for qRT-PCR. Reactions were performed using a Step One Plus Applied Biosystems thermocycler (Life Technologies) with the following protocol: First stage: 1 cycle of 4.14 °C/s up to 95 °C for 20 s; Second Stage: 40 cycles of 95 °C for 1s and 3.17°C/s down to 60 °C for 20s. The number of cycles necessary for the fluorescent intensity to increase exponentially, Ct values, were recorded and normalized to GAPDH expression for Chick DRGs and β -actin for rat Schwann cells. The comparative ΔCt method[176] was used to analyze the mRNA expression levels

of GDNF treated and untreated dissociated DRGs. Fold differences in relative mRNA expression levels over the control cultures were reported for each gene (n = 3 for all groups).

3.3.7 Western Blotting:

Proteins from dissociated DRGs were harvested with radioimmunoprecipitation assay buffer (RIPA buffer, 150mM sodium chloride, 1% Triton X-100, 0.5% Sodium deoxycholate, 0.1% SDS, 50mM Tris, pH 8.0) with protease inhibitor cocktail (Thermo Fisher). The protein concentration of the solution was determined using a Bradford protein assay (Thermo Fisher), and equal volumes of 2x Laemmli sample buffer were added. The samples were boiled for 5 minutes at 95 °C, and β-mercaptoethanol (10%, Life Technologies) was added before running on 4%–15% mini-PROTEAN TGX gradient gels (Bio-Rad, Hercules, CA) at 100 V for 1.5 hours. The western transfer was performed using the Trans-Blot Turbo Transfer System (Bio-Rad). The membrane was then probed with the following antibody dilutions overnight: SLITRK4 1:1000 (ab67308, Abcam, Cambridge, MA) and GAPDH 1:1000 (GA1R, Thermo Fisher). Rabbit anti-mouse (ab97046, Abcam) and goat anti-rabbit (ab6721, Abcam) horseradish peroxidase-conjugated secondary antibodies were used at a dilution of 1:25,000 and 1:1500 respectively and were incubated for 1 hour at room temperature before imaging using the UVP GelDoc-It^2® (Analytik Jena, CA, USA) imaging system.

3.3.8 Statistical Analysis:

One-way ANOVA was performed on the sample groups using Minitab software. Bonferroni posthoc test with $p<0.05$ for significance was used. Data represented were shown as mean ± standard deviation. Data included N = 8 or more devices per condition; n=30-518 neurites measured per device.

3.4 Results

3.4.1 Axon entrapment caused by GDNF-overexpressing Schwann cells (G-SCs) cannot be overcome by distal G-SCs

Our previous studies showed that G-SCs could cause trapping both *in vitro* and *in vivo* [6,7,175]. In this study, we wanted to examine whether entrapment by G-SCs can be overcome by cues distal to the G-SCs. Compared to seeding normal SCs in the middle chamber and no GDNF in the distal chamber (SC/-, 59.3±12.3% crossing), all conditions with G-SCs seeded in the middle chamber resulted in axon entrapment (G-SC/-, G-SC/SC, G-SC/G-SC, Fig. 3.2). More importantly, normal SCs or G-SCs seeded the in the distal chamber did not significantly improve axons crossing the middle chamber (G-SC/SC, 29.4±7.3% and G-SC/G-SC, 33.4±18.5% crossing, respectively) when entrapment occurred with G-SCs in the middle chamber. This result is similar to the effect of soluble GDNF has on axons, where high GDNF levels in the distal chamber cannot overcome axon entrapment caused by high GDNF levels in the middle chamber [175].

3.4.2 Axon entrapment caused by pre-conditioned SCs can be reduced by high GDNF levels or G-SCs in the distal chamber

Different SC phenotypes can impact the regeneration process. It has been shown that motor nerves repaired with sensory nerve grafts can impair the regeneration process [46,177]. We and others have shown that pre-conditioning SCs with GDNF can overcome sensory or motor SC phenotypic memory and improve regeneration with mismatched combinations of neurons and SCs (e.g., motor neurons with sensory SCs) [126,178]. This result led us to investigate whether pre-conditioning SCs with high GDNF concentrations can also induce SCs to cause trapping. We found that pre-conditioning SCs with 700 ng/mL of GDNF can significantly increase trapping (preSC700/-,

22.6±15.1% crossing) compared to untreated SCs (SC/-, 59.3±12.3% crossing) (Fig. 3.3C). Adding 100 ng/mL of GDNF in the distal chamber did not overcome this effect (preSC700/100, 29.2±6.1% crossing, Fig. 3.3C). However, both applying G-SCs or 700 ng/mL of GDNF in the distal chamber can overcome trapping (preSC700/G-SC, 67.5±16.4% crossing, and preSC700/700, 54.5±22.4% crossing, Fig. 3.3C). Applying 700 ng/mL of GDNF in the middle chamber after SCs pre-conditioning with no GDNF in the distal chamber did not overcome trapping with axons crossing at 28.5±16.3% (preSC700Cont700), which was significantly different from all groups except preSC700/- and preSC700/100 (Fig. 3.3C).

3.4.3 SLITRK4 is involved in axon entrapment induced by GDNF

Previously, we showed that high levels of soluble GDNF alone are sufficient to cause axon entrapment *in vitro* [174]. To understand how GDNF is able to negatively influence

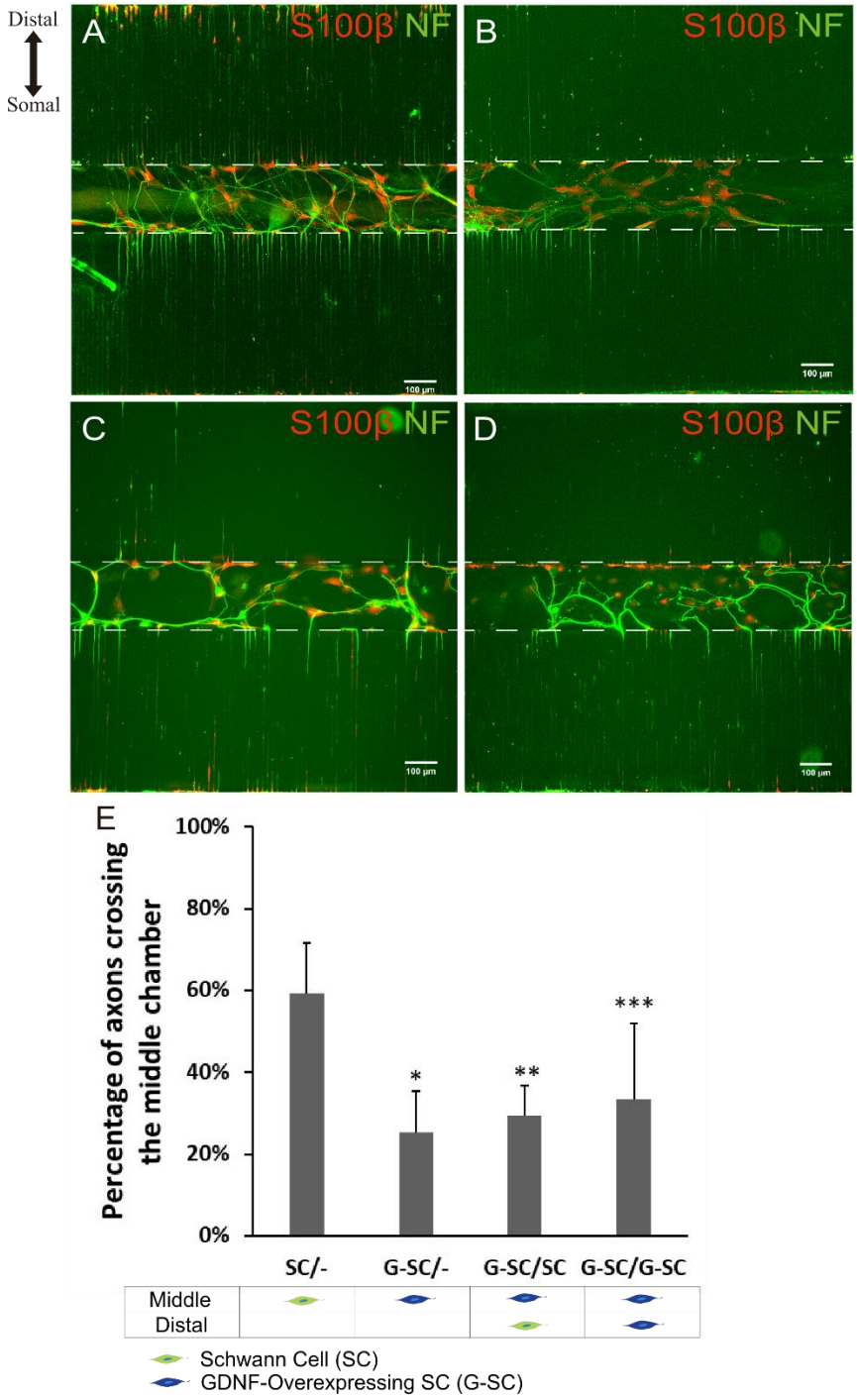

Figure 3.2: GDNF-Overexpressing Schwann Cells cannot overcome trapping in the middle chamber. A-B) Normal SCs seeded in the middle chamber promoted axon growth and axons crossing the middle chamber (A) whereas G-SCs seeded in the middle chamber impeded axons crossing (B). Normal SCs (C) and G-SCs (D) seeded in the distal chamber cannot overcome trapping caused by G-SCs in the middle chamber. E) Quantifications of axons crossing. N = 8. *: $p<0.0005$, **: $p<0.005$, ***: $p<0.01$ compared to SC/- condition.

axon growth, we performed DNA microarray analysis on dissociated DRGs treated with 0 or 700ng/mL of GDNF for 7 days. There were 101 differentially expressed genes with 36 up-regulated and 65 down-regulated (Fig. 3.4A). A list of genes refined by literature is presented (Fig. 3.4B). The complete list of differentially expressed genes is provided in the supplementary data (Table S3.1). These genes are at least 2 fold increased or decreased in expression and are known to be related to axonal guidance and outgrowth. In particular, SLIT and NTRK like family member 4 (SLITRK4) and protein tyrosine phosphatase receptor type O (PTPRO) have been shown to affect axon guidance and outgrowth. SLITRK family proteins are known to regulate neurite outgrowth [179]. PTPRO is expressed in $TrkB^+$ and Ret^+ DRG neurons and serves as a negative regulator of GDNF signaling [180]. To verify the DNA microarray results for these two genes, we used qRT-PCR to evaluate the mRNA levels of the genes (Fig. 3.4C). *SLITRK4* showed an increase of 6-fold compared to untreated DRGs while *PTPRO* showed a greater than 2-fold increase. Based on its role in axon growth and higher expression level, we decided to further investigate the role of *SLITRK4* in axon entrapment.

We used short-hairpin RNA vectors for SLITRK4 delivered through lentivirus to knock down the gene expression in neurons cultured in the microfluidic device to examine the effects on axon entrapment. The SLITRK4 knock-down group showed significantly higher axons crossing (56.6±21.2% crossing) than the trapping control (22.6±11.5% crossing, treated only with 700ng/mL of GDNF in the middle chamber) and the scrambled shRNA groups (34.2±8.3% crossing, Fig. 3.5A-D). The knockdown was confirmed through protein expression by Western blotting (Fig. 3.5E & F). In addition, we selected two inhibition targets downstream of SLITRK4 signaling, protein tyrosine phosphatase σ (PTP σ) and phospholipase C (PLC) to further verify the function of SLITRK4. The SLITRK family has been shown to interact with PTP type receptors

[181,182]. Specifically, SLITRK4 interacts with PTP σ. Using the PTP IV inhibitor, we examined the effects of PTP inhibition on axon entrapment. Y791 in TrkA show some degree of homology with the cytoplasmic tail of SLITRKS, Y945, raising the question of whether SLITRKS are also implicated in PLC-γ signaling [179]. Therefore, we used a PLC inhibitor, U73122, in an attempt to reduce axon entrapment.

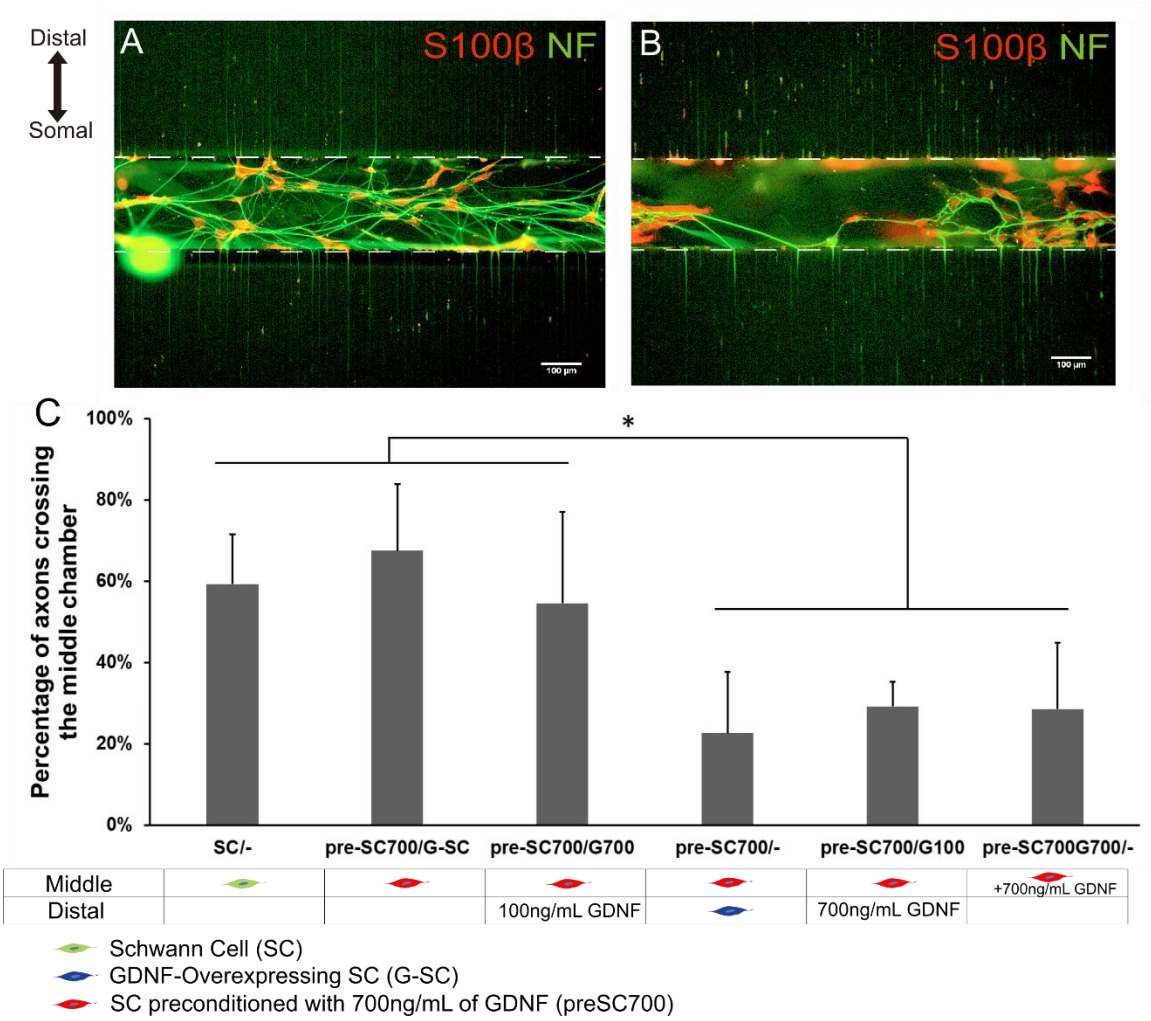

Figure 3.3: GDNF pre-conditioned SCs show trapping that is reversible. A) Untreated SCs did not show trapping whereas SCs pre-conditioned with 700ng/mL of GDNF (B) showed trapping. C) More importantly, this trapping can be reversed by 700ng/mL of GDNF or G-SCs in the distal chamber (preSC700/G-SC & preSC700/700). N=8. *: $p<0.05$.

PTP IV inhibitor significantly increased axons crossing (38.8±8.7% crossing) compared to the trapping control; whereas U73122 did not improve axons crossing (34.8±15.9% crossing).

3.5 Discussion

GDNF is an important component in nerve regeneration, affecting both neurons and SCs. It is known to attract axons, promote neuronal survival, and improve remyelination of regenerating axons [122–124,148,183]. At the same time, GDNF has been shown to directly affect SC proliferation, migration, and differentiation, all of which are essential steps of the axonal regeneration processes [124,170,184,185]. However, the window of endogenous GDNF release by the SCs is often too short for distal nerve injuries due to chronic denervation, leading to inadequate recovery [30]. Although gene therapy through adeno- and lentiviral mediated transductions prolongs GDNF release for the entire regeneration process, we and others have found that the overexpression of GDNF can severely reduce axonal growth and cause axon entrapment, leading to the "candy-store" effect [6,8,9,175]. The mechanism underlying the "candy-store" effect is still unknown. In our previous study, we developed an *in vitro* culture platform that aims to dissect this phenomenon by individually testing the possible factors that cause axon entrapment [175]. In this study, we further examined the effects of GDNF on SCs' ability to promote axon growth, as well as the molecular pathways in neurons activated by high GDNF levels.

Here, we showed that both SCs and G-SCs in the distal chamber could not overcome trapping caused by GDNF-overexpressing SCs in the middle chamber (Fig. 3.2).

A

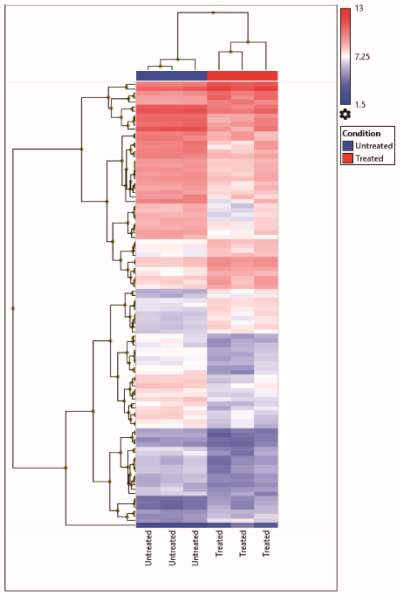

B

Gene	Fold Change
SLIT and NTRK like family member 4	2.35
Protein tyrosine phosphatase receptor type O	2.16
Villin like	2.12
Ret proto-oncogene	2.27
Transcription factor AP-2 beta	2.47
Contactin 4	2.08
Cerebellin 2 precursor	2.54
UDP-galactose ceramide galactosyltransferase	2.29
Vitrin	2.29
Heart and neural crest derivatives expressed 2	2.06
EGF containing fibulin-like ECM protein 1	-3.99
Integrin subunit beta-like	-3.88
Protocadherin-11 X-linked-like	-3.24
Growth differentiation factor 10	-2.69

C

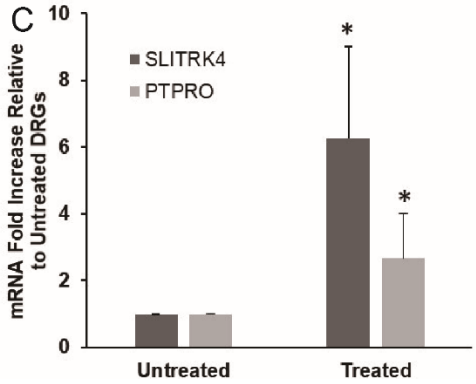

Figure 3.4: Gene expression differences between dissociated DRGs that are untreated or treated with 700ng/mL of GDNF. A) Differential gene expression analysis (data inclusion criteria: fold change > |2|, $p<0.05$) Statistical analysis: Benjamini-Hocherg procedure. B) Selected gene lists based on fold change and relationship to axonal guidance and outgrowth. C) qRT-PCR of SLITRK4 and PTPRO relative to untreated DRGs. N=3, *: $p<0.05$ compared to untreated groups.

These results were similar to axon entrapment caused by high levels of soluble GDNF alone. High levels of GDNF in the distal chamber were not able to overcome trapping in the middle chamber [175]. Interestingly, we found pre-conditioned SCs with high levels of GDNF can also cause trapping. However, the entrapment was reversible by either seeding G-SCs or applying

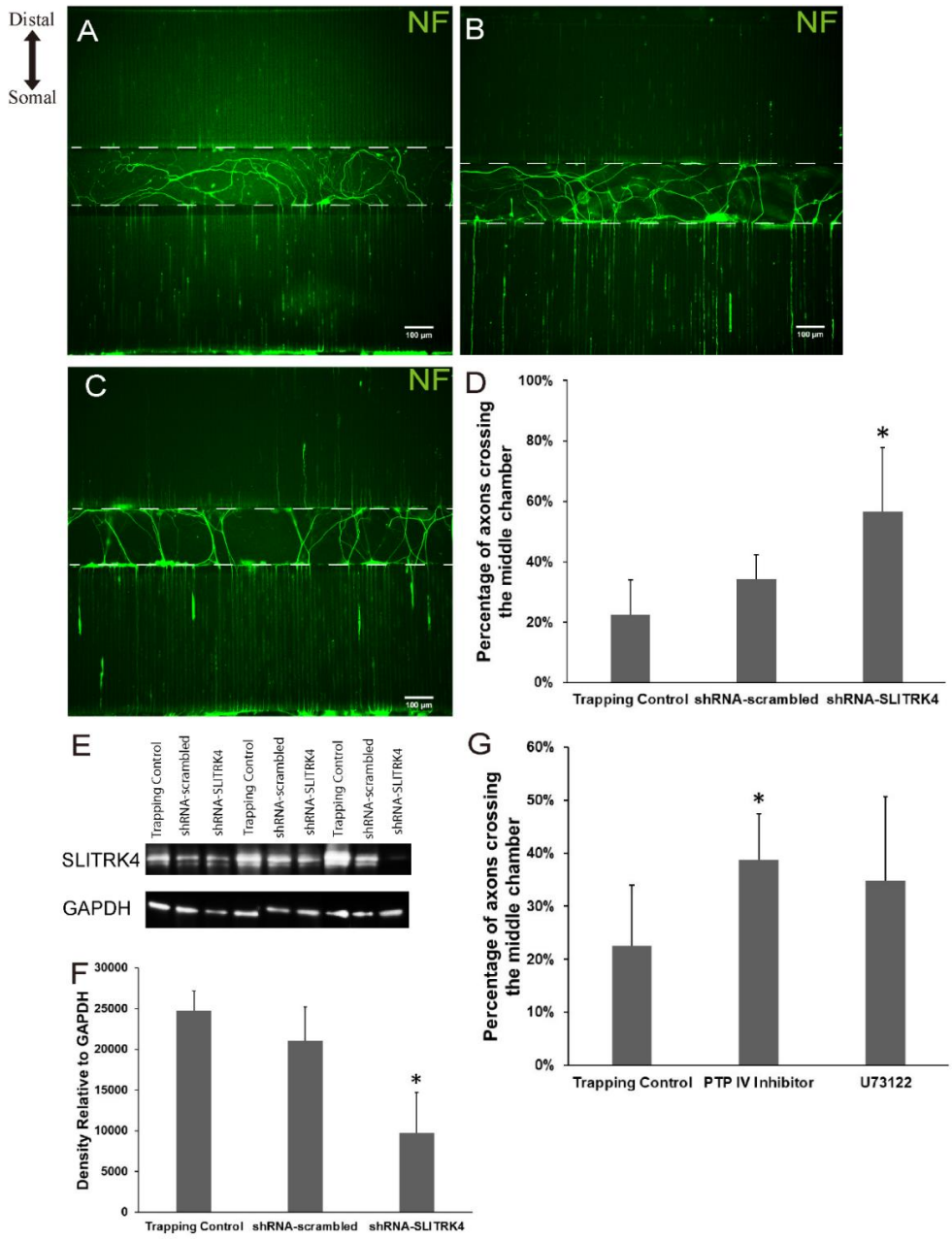

Figure 3.5: SLTITRK4 shRNA knockdown on dissociated DRGs. A-C) Immunocytochemistry staining of neurofilaments on dissociated DRGs treated with 700 ng/mL of GDNF. A) Trapping control treated with 700ng/mL of GDNF but no shRNA. B) Scrambled shRNA that should not silence SLITRK4. C) SLITRK4-shRNA treated. D) Quantifications of axons crossing the middle chamber of the knockdown study. N = 11-16, *: $p<0.005$. E) Western blot analysis of SLITRK4 protein with GAPDH as control F) Densitometry of the Western blot SDS-PAGE gel. N = 3, *: $p<0.05$. G) Quantifications of axons crossing the middle chamber where DRGs are treated with inhibitors of PTP (PTP IV inhibitor) and Phospholipases C (U73122). N = 8, *: $p<0.05$ compared to positive control.

700

ng/mL of GDNF in the distal chamber. These results may indicate that GDNF-induced axon entrapment is irreversible with continuously high GDNF treatment. In contrast, preconditioning SCs with GDNF induced axon entrapment that can be reversed with high GDNF sources distal to the SCs. It has been shown that GDNF treatment of SCs can induce a positive feedback pathway that allows SCs to secrete more GDNF [122,126]. Based on the results of the current study, pre-conditioned SCs might cause axon entrapment through endogenous GDNF production by the SCs. However, such GDNF level might not be sufficient to cause more permanent trapping and can be overcome by high levels downstream. Marquardt *et al*. showed that by temporally controlling GDNF release, various degrees of axon growth was achieved [6]. With 8 weeks of continuous GDNF release, axon entrapment occurred *in vivo*; 4 weeks of GDNF release was not sufficient for axons to cross the 30 mm sciatic nerve defect in rats; while 6 weeks of GDNF release allowed for axons to cross the injury gap and did not cause axon entrapment. These results together seem to suggest the duration of high levels of GDNF can determine whether the effect on axons is beneficial or detrimental.

Ee *et al*. have shown that G-SCs have a distinct gene expression profile compared to normal SCs [156]. One of the highly expressed gene target neuropeptide Y (NPY) is well studied and is known to be involved in axon growth. We examined its effects on axon growth in our device, but the results did not show any axon entrapment when applied in high concentrations (data not shown). We also examined whether applying high levels of GDNF to pre-conditioned SCs would further increase axon entrapment (Fig. 3.3C, preSC700Cont700). We did not observe any increase in axon entrapment, which may suggest the effects of pre-conditioned SCs trapping neurites and GDNF trapping neurites were not additive. We and others have shown that GDNF overexpression can cause the formation of irregular fiber networks at GDNF depot [8,130,156,175]. Specifically, G-SCs can

cause accumulation of axons, as well as irregular axon sprouting while normal SCs did not. This might be attributed to the interaction of G-SCs with fibroblasts, which can result in significantly ECM remodeling [156]. Interestingly, SCs pre-conditioned with high levels of GDNF also demonstrated similar characteristics. While both untreated SCs and SCs pre-conditioned with low levels of GDNF showed relatively smooth neurites growing along them, both G-SCs and SCs pre-conditioned with high levels of GDNF showed neurites with more sharp turns or kinks (Fig. 3.2A-D and Fig.3A-B). In contrast, even though soluble GDNF can cause axon entrapment, it did not show similar fiber network formation [175]. Together, these results suggest GDNF and SCs constitute as different components of the "candy-store" effect.

To further understand how GDNF can affect neurite outgrowth, we analyzed the gene expression profile of dissociated DRGs treated with high GDNF. Through screening, we identified *SLITRK4* as a likely candidate that may contribute to the axon entrapment. The SLITRK family proteins have been implicated in controlling axon outgrowth, promoting neuronal survival, and forming synapses [179,186,187]. Initial studies have shown that expression of SLITRKs in PC12 cells can decrease the number of neurites with NGF treatment [179]. Further investigations show that SLITRK1 can improve the dendritic length of the cortical neurons *in vitro* [186]. Similarly, SLITRK5-knockout mice showed a marked decrease in dendritic complexity of medium spiny neurons in the striatum [187]. With selectively high expression in the inner ear, SLITRK6 promotes the survival and neurite outgrowth of sensory neurons of the inner ear [188]. Interestingly, Slitrk6-knockout mice showed decreased protein levels of TrkB and TrkC, which suggests a role in modulating the neurotrophin signaling pathway. Common to all SLITRK family proteins are the leucine-rich repeats (LRR). Linx, for example, is an LRR and immunoglobulin family protein that interacts with Ret, which is the receptor of GDNF in neurons [189]. While no previous studies have

investigated the direct link between GDNF and *SLITRK4*, our findings showed that high GDNF could increase *SLITRK4* gene expression.

All six Slitrks are also synaptogenic, as demonstrated by artificial synapse-formation assay [190,191]. With the exception of SLITRK3, which is specifically localized to inhibitory synapse and interact with presynaptic protein tyrosine phosphatase δ (PTPδ), all other SLITRK proteins are involved in excitatory synapse formation and interact with PTPσ [190,191]. Based on this result, we wanted to examine whether inhibiting PTPσ can affect SLITRK4 signaling pathway. Our results indicate that using PTP IV inhibitor can reduce axon entrapment. This further strengthens the relationship between SLITRK4 and axon entrapment. Another gene target that was upregulated in our DNA microarray assay was *PTPRO,* which is involved in excitatory synapse formation [192]. Many studies have shown that GDNF not only promotes axon growth but also synapse formation. In a seminal study, Ledda *et al*. showed GDNF and its receptor, GFRα1 promote synapse formation by ligand-induced cell adhesion [193]. Together, these findings suggest that GDNF can form both direct cell-cell interactions as well as increase the expressions of other genes, such as *SLITRK4* and *PTPRO*, to promote synapse formation.

In this study, we investigated how high levels of GDNF can impact SCs ability to promote axon growth and the underlying mechanisms by which GDNF can cause axon entrapment. We showed that axon entrapment by G-SCs could not be overcome with other sources of high levels of GDNF, including G-SCs. In contrast, axon entrapment caused by SCs pre-conditioned with high GDNF levels can be rescued by distal sources of high GDNF. Through gene expression analysis and gene-silencing studies, we were able to demonstrate that *SLITRK4* plays an important role in axon entrapment. In conclusion, these results may prove valuable in understanding the effects of

GDNF on both SCs and neurons, providing guidance towards developing better GDNF delivery methods to establish a potential therapeutic for PNI.

3.6 Supplementary Data

Table S3.1 Complete List of Differentially Expressed Genes in Dissociated DRGs Treated with 700ng/mL of GDNF

Gene Symbol	Fold Change	FDR P-val	Description
KCNS3	3.92	0.0136	potassium voltage-gated channel, modifier subfamily S, member 3
SPP1; PKD2	3.45	0.1062	secreted phosphoprotein 1; polycystic kidney disease 2 (autosomal dominant)
HS3ST1	3.38	0.0863	heparan sulfate (glucosamine) 3-O-sulfotransferase 1
LOC423822	3.36	0.0308	heparan sulfate glucosamine 3-O-sulfotransferase 1-like
TMEM233	2.89	0.0136	transmembrane protein 233
PLCL1	2.87	0.0353	phospholipase C-like 1
C17ORF58	2.87	0.0148	chromosome 18 open reading frame, human C17orf58
LOC395159	2.77	0.1046	Schwann cell-specific EGF-like repeat autocrine factor
BCO2	2.75	0.1117	beta-carotene oxygenase 2
CBLN2	2.54	0.0218	cerebellin 2 precursor
TFAP2B	2.47	0.0154	transcription factor AP-2 beta (activating enhancer binding protein 2 beta)
PLCXD2	2.46	0.0613	phosphatidylinositol-specific phospholipase C, X domain containing 2
SERTM1	2.38	0.0447	serine-rich and transmembrane domain containing 1
DLGAP2	2.37	0.0791	discs, large (Drosophila) homolog-associated protein 2
SLITRK4	2.35	0.0136	SLIT and NTRK-like family, member 4
UGT8	2.29	0.0136	UDP glycosyltransferase 8
VIT	2.29	0.0451	vitrin
RET	2.27	0.0136	ret proto-oncogene
CACNG2	2.27	0.0757	calcium channel, voltage-dependent, gamma subunit 2
SOSTDC1	2.22	0.1909	sclerostin domain containing 1
LIPG	2.19	0.2019	lipase, endothelial
PTPRO	2.16	0.0579	protein tyrosine phosphatase, receptor type, O
TMEM163	2.12	0.0319	transmembrane protein 163
VILL	2.12	0.1644	villin-like
PTPRT	2.11	0.0218	protein tyrosine phosphatase, receptor type, T
SV2B	2.09	0.0234	synaptic vesicle glycoprotein 2B
LOC101750415	2.09	0.1646	uncharacterized LOC101750415
CNTN4	2.08	0.0248	contactin 4
ATP6AP1L	2.06	0.0447	ATPase, H+ transporting, lysosomal accessory protein 1-like
HAND2	2.06	0.1164	heart and neural crest derivatives expressed 2

MAB21L1	2.05	0.0428	mab-21-like 1 (C. elegans)
KCNA1	2.05	0.0295	potassium voltage-gated channel, shaker-related subfamily, member 1 (episodic ataxia with myokymia)
GRPR	2.02	0.1097	gastrin-releasing peptide receptor
VLDLR	2.01	0.0381	very low density lipoprotein receptor
SLITRK4	2.01	0.0148	SLIT and NTRK-like family, member 4
CHAT	2	0.0218	choline O-acetyltransferase
CHODL	-2.04	0.2272	chondrolectin
C10ORF112	-2.04	0.0428	chromosome 2 open reading frame, human C10orf112
CSRP1	-2.05	0.042	cysteine and glycine-rich protein 1
LOC422513	-2.06	0.1919	hect domain and RLD 4-like
TNFRSF1B	-2.06	0.0604	tumor necrosis factor receptor superfamily, member 1B
SLC2A12	-2.07	0.0319	solute carrier family 2 (facilitated glucose transporter), member 12
SELENBP1; LOC100857226	-2.08	0.232	selenium binding protein 1; selenium-binding protein 1-A-like
PODN	-2.08	0.0715	podocan
DSC2	-2.1	0.0455	desmocollin 2
TLR3	-2.11	0.0977	toll-like receptor 3
SLC38A4	-2.11	0.0353	solute carrier family 38, member 4
MCTP1	-2.12	0.0727	multiple C2 domains, transmembrane 1
FIBIN	-2.12	0.1217	fin bud initiation factor homolog (zebrafish)
MYLK	-2.12	0.0926	myosin light chain kinase
BBOX1	-2.13	0.0578	butyrobetaine (gamma), 2-oxoglutarate dioxygenase (gamma-butyrobetaine hydroxylase) 1
PRRX1	-2.13	0.0839	paired related homeobox 1
VIP	-2.14	0.0525	vasoactive intestinal peptide
IL1RL1	-2.14	0.0451	interleukin 1 receptor-like 1
PALMD	-2.16	0.0248	palmdelphin
CDC42EP3	-2.17	0.0562	CDC42 effector protein (Rho GTPase binding) 3
MYL9	-2.18	0.0674	myosin, light chain 9, regulatory
AVPR2	-2.18	0.1221	arginine vasopressin receptor 2
LMO7	-2.25	0.0525	LIM domain 7
FAM83B	-2.25	0.1385	family with sequence similarity 83, member B
PID1	-2.27	0.1498	phosphotyrosine interaction domain containing 1
PDGFD	-2.29	0.0218	platelet derived growth factor D
FAM180A	-2.31	0.12	family with sequence similarity 180, member A
COLEC10	-2.31	0.1252	collectin sub-family member 10 (C-type lectin)
ERG	-2.33	0.0319	v-ets avian erythroblastosis virus E26 oncogene homolog
MYH1D	-2.35	0.1282	myosin, heavy chain 1D, skeletal muscle (similar to human myosin, heavy chain 1, skeletal muscle, adult)

RIPK3	-2.43	0.0218	receptor-interacting serine-threonine kinase 3
MYL10	-2.44	0.0639	myosin, light chain 10, regulatory
PENK	-2.47	0.0218	proenkephalin
SVEP1	-2.51	0.0356	sushi, von Willebrand factor type A, EGF and pentraxin domain containing 1
FHL2	-2.52	0.219	four and a half LIM domains 2
NEDD9	-2.58	0.0439	neural precursor cell expressed, developmentally down-regulated 9
LOC396531	-2.59	0.0608	parvalbumin
ACTC1	-2.61	0.0493	actin, alpha, cardiac muscle 1
CYTL1	-2.61	0.0795	cytokine-like 1
MYL1	-2.63	0.0538	myosin, light chain 1, alkali; skeletal, fast
PRRX2	-2.65	0.0921	paired related homeobox 2
SIK1	-2.67	0.0218	salt-inducible kinase 1
GDF10	-2.69	0.0791	growth differentiation factor 10
PKP2	-2.86	0.12	plakophilin 2
ENPP3	-2.88	0.0596	ectonucleotide pyrophosphatase/phosphodiesterase 3
STEAP1	-3.01	0.0519	six transmembrane epithelial antigen of the prostate 1
PDLIM3	-3.04	0.0202	PDZ and LIM domain 3
SLCO2A1	-3.05	0.0863	solute carrier organic anion transporter family, member 2A1
SLC39A8	-3.15	0.0552	solute carrier family 39 (zinc transporter), member 8
KCNMB1	-3.15	0.0854	potassium channel subfamily M regulatory beta subunit 1
A2ML3; A2M	-3.17	0.0418	alpha-2-macroglobulin-like 3; alpha-2-macroglobulin
MMP27	-3.19	0.0356	matrix metallopeptidase 27
PDPN	-3.2	0.0202	podoplanin
LOC422264	-3.24	0.0579	protocadherin-11 X-linked-like
KRT15	-3.27	0.3031	keratin 15
KRT19	-3.45	0.0326	keratin 19
NEXN	-3.79	0.1058	nexilin (F actin binding protein)
ITGBL1	-3.88	0.1015	integrin, beta-like 1 (with EGF-like repeat domains)
OMD; ASPN	-3.96	0.0353	osteomodulin; asporin
EFEMP1	-3.99	0.0525	EGF containing fibulin-like extracellular matrix protein 1
STEAP1	-4.08	0.0761	six transmembrane epithelial antigen of the prostate 1
PAWR	-4.23	0.0609	PRKC, apoptosis, WT1, regulator
NOV	-5.19	0.0525	nephroblastoma overexpressed
COCH	-5.98	0.1607	cochlin
C7	-8.01	0.1897	complement component 7

Chapter 4: Summary of Findings and Future Directions

4.1 Summary of Findings

This body of work has sought to elucidate the mechanism of the "candy-store" where high levels of GDNF can affect both the SCs and neurons. The results shown in this thesis suggest that high levels of soluble GDNF alone are sufficient to cause the "candy-store" effect and that Slitrk4 is involved in the process of axon entrapment. Consistent with the *in vivo* results, GDNF-overexpressing SCs also induced axon entrapment *in vitro*. In addition to axon entrapment, dense fiber networks formed along GDNF-overexpressing SCs. These results suggest that the "candy-store" effects consist of two parts, where axon trapping is caused by GDNF directly, and fiber networks form in the presence of GDNF-overexpressing SCs. These results were found through two studies whose objectives included: to develop a culture platform that can recapitulate axon entrapment *in vitro*; to evaluate the effects of supra-physiological concentrations of GDNF on axon entrapment and SC response.

The first study of this thesis developed an *in vitro* platform that can be used to model axon entrapment observed with high GDNF from transgenic overexpression seen in previous *in vivo* studies. The three-chamber culture platform allowed neurons to be seeded in one end chamber while the effect of various trapping conditions in the other two chambers was used to study neurite entrapment. Firstly, we verified that GDNF-overexpressing SCs could cause axon entrapment *in vitro.* It was also found that supra-physiological levels of GDNF alone were sufficient to induce axon entrapment. Moreover, equally high levels of GDNF distal to the entrapment sites cannot overcome such an effect. Importantly, soluble GDNF did not cause axon coil formation suggesting two separate roles of GDNF and SCs in contributing to the "candy-store" effect.

The second study of this thesis focused on understanding whether GDNF is affecting the neurons directly or SCs affected by GDNF are causing axons to trap. Similar to soluble GDNF, GDNF-overexpressing SCs can induce axon entrapment that cannot be reversed by distal sources of high GDNF. In contrast, while pre-conditioning SCs in high levels of GDNF can also cause axon entrapment, such effect can be reduced by distal sources of high GDNF levels. When evaluating the direct effects of GDNF on neurons, we found that SLITRK4 was significantly upregulated when dissociated DRGs are treated with high concentrations of GDNF. It was confirmed through SLITRK4-shRNA knock-down studies, that axon entrapment was significantly reduced. Furthermore, inhibition of SLITRK4 ligand, PTPσ also reduced axon entrapment and further verified the role of SLITRK4 in causing axon entrapment when treated with high concentrations of GDNF.

4.2 Future Directions

4.2.1 Understanding the Roles of GDNF in Affecting SCs

Findings of this work highlight the importance of GDNF's effects on SCs. Our results showed that GDNF-overexpressing SCs *in vitro* were able to demonstrate similar effects to that of *in vivo*. Besides axon entrapment, the formation of axon coils was also present with GDNF-overexpressing SCs. This morphology was absent when neurons are treated with soluble GDNF, suggesting the importance of SC-axon interactions. SCs were shown to closely interact with their surrounding microenvironment, including axons and fibroblasts, through cell-cell signaling [194]. In addition, GDNF overexpression can significantly alter the gene expression of SCs [123,156]. Therefore it might be important to study the presence of cell membrane proteins and understand how they might affect axon guidance and induce axon coil formation. Another potential interaction of SCs with its microenvironment might be SCs remodeling the surrounding ECM, which may cause the

formation of axon coils. Ee *et al*. showed that the interaction between G-SCs and fibroblast could significantly affect the surrounding ECM [156]. It would be interesting to understand whether the remodeled ECM can also affect axon guidance and axon coil formation.

The results of the second study indicated that axon entrapment caused by SCs pre-conditioned with high GDNF could be reversed by distal sources of high GDNF. In contrast, both soluble GDNF and G-SCs induced axon entrapment that cannot be overcome. These results seem to suggest that the constitutive presence of high GDNF levels can induce more permanent trapping compared to pre-conditioned SCs. It is known that GDNF can induce the production of GDNF in SCs through a positive feedback loop [122]. Therefore, it might be worth investigating the levels of GDNF production in SCs pre-conditioned with high GDNF concentrations to better understand the differences in GDNF levels between permanent and non-permanent trapping. This might help develop better strategies that optimize GDNF release to prevent permanent axon entrapment.

4.2.2 Combining SLITRK4 Inhibition with GDNF Overexpression for Nerve Regeneration

This body of work has demonstrated that high levels of GDNF treatment can increase SLITRK4 expression. Many SLITRK family proteins, except SLITRK4, demonstrated roles in synapse formations [179]. While the exact functions of SLITRK4 are unknown, the leucine-rich repeats (LRR) of the protein may be involved in modulating the neurotrophin signaling pathways through TrkB and TrkC [188]. Linx, an LRR protein, has been demonstrated to interact with Ret, which is a GDNF receptor expressed in neurons [189]. Many studies have also shown that GDNF can significantly increase muscles innervation through synapse formation at neuromuscular junctions [119,195]. Our studies suggest that GDNF is involved in the regulation of SLITRK4 expression. It may be valuable to know the molecular pathway of how one protein is affecting the other. By interfering

with such signaling pathway, we may be able to reduce the trapping effect of GDNF overexpression and only harness its beneficial effect of promoting axonal growth. In addition, the functions of SLITRK4 can be further elucidated.

This thesis also demonstrated that the knock-down and inhibition of SLITRK4 could reduce axon entrapment *in vitro*. Future studies using animal models can be used to investigate the combined effects of GDNF overexpression and SLITRK4 inhibition. Either by transplanting GDNF-overexpressing SCs in a scaffold or directly injecting GDNF overexpression transduction viral vectors at the site of injury, inhibition of SLITRK4 through shRNA could be delivered at the same time to examine whether axon entrapment still occurs. Alternatively, inhibition of PTPσ can be easily achieved by incorporating the inhibitors in the scaffold where the G-SCs were seeded. By assessing the number of axons that could grow pass the GDNF depot, we could evaluate the efficiency of such combinatory therapy in treating peripheral nerve injury in animal models.

4.2.3 Alternative Strategies of Controlled GDNF Delivery

Another approach for better using the potent effects of GDNF is through controlled release of GDNF. Previously, our lab has experimented the using of the doxycycline-controlled release of GDNF *in vivo* [6]. It was shown that 4 weeks of GDNF release was insufficient for axon regeneration, 8 weeks of GDNF release resulted in the "candy-store" effect, and 6 weeks of GDNF release achieved the best axon regeneration while avoided axon entrapment. This result highlighted the advantage of controlled release compared to constitutive overexpression. The results of the current thesis showed that axon entrapment caused by SCs pre-conditioned with high GDNF could be non-permanent. Potential strategies can be developed to use the inducible release of GDNF at a non-permanent trapping level. This will enable the repair scaffold to present the strongest signals to the regeneration axons while avoiding the negative effect of permanent axon entrapment.

Selecting different locations for GDNF overexpression should also be considered. Previous studies showed that GDNF overexpression from muscle had a better effect on nerve regeneration than central delivery from GFAP-expressing cells [185,196]. Since muscle cells are the final targets for the motor neuron in PNS, myoblast might be a potential candidate for GDNF overexpression, especially if the injury site is close enough to the overexpression site for axons to sense the trophic effect.

References

1. Webber, C. & Zochodne, D. The nerve regenerative microenvironment: Early behavior and partnership of axons and Schwann cells. *Exp. Neurol.* **223**, 51–59 (2010).
2. Grinsell, D. & Keating, C. P. Peripheral Nerve Reconstruction after Injury: A Review of Clinical and Experimental Therapies. *Biomed Res. Int.* **2014**, (2014).
3. Springer, J. E. *et al.* cDNA sequence and differential mRNA regulation of two forms of glial cell line-derived neurotrophic factor in Schwann cells and rat skeletal muscle. *Exp Neurol* **131**, 47-52. ST-cDNA sequence and differential mRNA r (1995).
4. Scheib, J. & Höke, A. Advances in peripheral nerve regeneration. *Nat. Rev. Neurol.* **9**, 668–76 (2013).
5. Wu-Fienberg, Y. *et al.* Viral transduction of primary Schwann cells using a Cre-lox system to regulate GDNF expression. *Biotechnol. Bioeng.* **111**, 1886–1894 (2014).
6. Marquardt, L. M. *et al.* Finely Tuned Temporal and Spatial Delivery of GDNF Promotes Enhanced Nerve Regeneration in a Long Nerve Defect Model. *Tissue Eng. Part A* **21**, 2852–64 (2015).
7. Santosa, K. B. *et al.* Nerve allografts supplemented with schwann cells overexpressing glial-cell-line-derived neurotrophic factor. *Muscle and Nerve* **47**, 213–223 (2013).
8. Blits, B. *et al.* Rescue and sprouting of motoneurons following ventral root avulsion and reimplantation combined with intraspinal adeno-associated viral vector-mediated expression of glial cell line-derived neurotrophic factor or brain-derived neurotrophic factor. *Exp. Neurol.* **189**, 303–316 (2004).
9. Tannemaat, M. R. *et al.* Differential effects of lentiviral vector-mediated overexpression of nerve growth factor and glial cell line-derived neurotrophic factor on regenerating sensory and motor axons in the transected peripheral nerve. *Eur. J. Neurosci.* **28**, 1467–1479 (2008).
10. Lundborg, G. Nerve injury and repair - A challenge to the plastic brain. in *Journal of the Peripheral Nervous System* **8**, 209–226 (2003).
11. Taylor, C. a, Braza, D., Rice, J. B. & Dillingham, T. The incidence of peripheral nerve injury in extremity trauma. *Am. J. Phys. Med. Rehabil.* **87**, 381–385 (2008).
12. Noble, J., Munro, C. A., Prasad, V. S. S. V. & Midha, R. Analysis of upper and lower extremity peripheral nerve injuries in a population of patients with multiple injuries. *J. Trauma - Inj. Infect. Crit. Care* (1998). doi:10.1097/00005373-199807000-00025
13. SELECKI, B. R., RING, I. T., SIMPSON, D. A., VANDERFIELD, G. K. & SEWELL, M. F. TRAUMA TO THE CENTRAL AND PERIPHERAL NERVOUS SYSTEMS PART II: A STATISTICAL PROFILE OF SURGICAL TREATMENT NEW SOUTH WALES 1977. *Aust. N. Z. J. Surg.* (1982). doi:10.1111/j.1445-2197.1982.tb06081.x
14. Robinson, L. R. Traumatic injury to peripheral nerves. *Muscle and Nerve* **23**, 863–873 (2000).
15. Eser, F., Aktekin, L., Bodur, H. & Atan, C. Etiological factors of traumatic peripheral nerve injuries. *Neurol. India* **57**, 434 (2009).
16. Robinson, L. R., Jarvik, J. G. & Kline, D. G. Assessment of Traumatic Nerve Injuries. in (American Association of Neuromuscular and Electrodiagnostic Medicine, 2005).
17. Reid, A. J., Shawcross, S. G., Hamilton, A. E., Wiberg, M. & Terenghi, G. N-Acetylcysteine alters apoptotic gene expression in axotomised primary sensory afferent subpopulations. *Neurosci. Res.* **65**, 148–155 (2009).

18. Lundborg, G. A 25-year perspective of peripheral nerve surgery: Evolving neuroscientific concepts and clinical significance. *J. Hand Surg. Am.* **25**, 391–414 (2000).
19. McKay Hart, A., Brannstrom, T., Wiberg, M. & Terenghi, G. Primary sensory neurons and satellite cells after peripheral axotomy in the adult rat. *Exp. Brain Res.* **142**, 308–318 (2003).
20. Waller, A. Experiments on the Section of the Glossopharyngeal and Hypoglossal Nerves of the Frog , and Observations of the Alterations Produced Thereby in the Structure of Their Primitive Fibres Author (s): Augustus Waller Source : Philosophical Transactions of th. *Philos. Trans. R. Soc. London* **140**, 423–429 (1850).
21. Stoll, G., Jander, S. & Myers, R. R. Degeneration and regeneration of the peripheral nervous system: From Augustus Waller's observations to neuroinflammation. *J. Peripher. Nerv. Syst.* **7**, 13–27 (2002).
22. Burnett, M. G., Zager, E. L., Urnett, M. A. R. K. G. B. & Ager, E. R. I. C. L. Z. Pathophysiology of peripheral nerve injury : a brief review. *Neurosurg. Focus* **16**, 1–7 (2004).
23. Jessen, K. R. & Mirsky, R. The origin and development of glial cells in peripheral nerves. *Nat. Rev. Neurosci.* **6**, 671–682 (2005).
24. Griffin, J. W. & Thompson, W. J. Biology and pathology of nonmyelinating schwann cells. *Glia* **56**, 1518–1531 (2008).
25. Hoffman-Kim, D., Mitchel, J. A. & Bellamkonda, R. V. Topography, Cell Response, and Nerve Regeneration. *Annu. Rev. Biomed. Eng.* **12**, 203–231 (2010).
26. Fontana, X. *et al.* C-Jun in Schwann cells promotes axonal regeneration and motoneuron survival via paracrine signaling. *J. Cell Biol.* **198**, 127–141 (2012).
27. Brushart, T. M. *et al.* Schwann cell phenotype is regulated by axon modality and central – peripheral location , and persists in vitro ☆ . **247**, 272–281 (2013).
28. Reichardt, L. Extracellular Matrix Molecules And Their Receptors: Functions In Neural Development. *Annu. Rev. Neurosci.* **14**, 531–570 (1991).
29. Weinberg, H. J. & Spencer, P. S. The fate of Schwann cells isolated from axonal contact. *J. Neurocytol.* 555–569 (1978).
30. Höke, A., Gordon, T., Zochodne, D. W. D. & Sulaiman, O. A. R. A decline in glial cell-line-derived neurotrophic factor expression is associated with impaired regeneration after long-term Schwann cell denervation. *Exp. Neurol.* **173**, 77–85 (2002).
31. You, S., Petrov, T., Chung, P. H. & Gordon, T. The Expression of the Low Affinity Nerve Growth Factor Receptor in. **100**, 87–100 (1997).
32. Anzil, A. P. & Wernig, A. Muscle fibre loss and reinnervation after long-term denervation. *J. Neurocytol.* 833–845 (1989).
33. Ma, C. H. E. *et al.* Accelerating axonal growth promotes motor recovery after peripheral nerve injury in mice. *J. Clin. Invest.* **121**, 4332 (2011).
34. Wood, M. D. *et al.* GDNF released from microspheres enhances nerve regeneration after delayed repair. *Muscle and Nerve* **46**, 122–124 (2012).
35. Madison, R. D., Archibald, S. J. & Brushart, T. M. Reinnervation Accuracy of the Rat Femoral Nerve by Motor and Sensory Neurons. **16**, 5698–5703 (1996).
36. Wigston, D. & Donahue, S. The location of cues promoting selective reinnervation of axolotl muscles. *J. Neurosci.* **8**, 3451–3458 (1988).
37. Ray, W. Z. & Mackinnon, S. E. Management of nerve gaps : Autografts , allografts , nerve transfers , and end-to-side neurorrhaphy. *Exp. Neurol.* **223**, 77–85 (2010).
38. Prasad, A. R., Steck, J. K. & Dellon, A. L. Zone of Traction Injury of the Common Peroneal

Nerve. **59**, 302–306 (2007).
39. Siemionow, M. & Brzezicki, G. *CURRENT TECHNIQUES AND CONCEPTS*. *International Review of Neurobiology* **87**, (Elsevier Inc., 2009).
40. Lundborg, G. & Rydevik, B. Effects of Stretching the Tibial Nerve of the Rabbit. *J. bone Jt. Surg.* **55B**, (1973).
41. Pfister, B. J. *et al.* Biomedical Engineering Strategies for Peripheral Nerve Repair : Surgical Biomedical Engineering Strategies for Peripheral Nerve Repair : Surgical Applications , State of the Art , and Future Challenges. *Crit. Rev. Biomed. Eng.* **39**, 81–124 (2011).
42. Mackinnon, S. E. & Dellon, A. L. *Surgery of the peripheral nerve*. (Thieme Medical Publishers, 1988).
43. Norkus, T., Norkus, M. & Ramanauskas, T. Donor , recipient and nerve grafts in brachial plexus reconstruction : anatomical and technical features for facilitating the exposure. *Surg. Radiol. Anat.* **27**, 524–530 (2005).
44. Colen, K. L., Choi, M. & Chiu, D. T. W. Nerve grafts and conduits. *Plast. Reconstr. Surg.* **124**, 386–394 (2009).
45. Moore, A. M. *et al.* Limitations of conduits in peripheral nerve repairs. *Hand* **4**, 180–186 (2009).
46. Brenner, M. J. *et al.* Repair of Motor Nerve Gaps With Sensory Nerve Inhibits Regeneration in Rats. *Laryngoscope* 1685–1692 (2006). doi:10.1097/01.mlg.0000229469.31749.91
47. Moradzadeh, A. *et al.* The impact of motor and sensory nerve architecture on nerve regeneration. *Exp. Neurol.* **212**, 370–376 (2008).
48. Brushart, T. M. Preferential reinnervation of motor nerves by regenerating motor axons. *J. Neurosci.* **8**, 1026–31 (1988).
49. Safa, B. & Buncke, G. Autograft Substitutes. Conduits and Processed Nerve Allografts. *Hand Clin.* **32**, 127–140 (2016).
50. Yu, L. T., Rostami, A., Silvers, W. K., Larossa, D. & Hickey, W. F. Expression of major histocompatibility complex antigens on inflammatory peripheral nerve lesions. *J. Neuroimmunol.* **30**, 121–128 (1990).
51. Hudson, T. W. *et al.* Optimized Acellular Nerve Graft Is Immunologically Tolerated and Supports Regeneration. *Tissue Eng.* (2004). doi:10.1089/ten.2004.10.1641
52. Johnson, P. J., Newton, P., Hunter, D. A. & MacKinnon, S. E. Nerve endoneurial microstructure facilitates uniform distribution of regenerative fibers: A post hoc comparison of midgraft nerve fiber densities. *J. Reconstr. Microsurg.* (2011). doi:10.1055/s-0030-1267834
53. Evans, P. J., MacKinnon, S. E., Levi, A. D. O., Hunter, D. A. & Midha, R. Cold Preserved Nerve Allografts : Changes in Basement Membrane , Viability ,. *Muscle Nerve* **21**, 1507–1522 (1998).
54. Gold, B. G., Katoh, K. & Storm-Dickerson, T. The immunosuppressant FK506 increases the rate of axonal regeneration in rat sciatic nerve. *J. Neurosci.* **15**, 7509–16 (1995).
55. Feng, F. Y. *et al.* FK506 rescues peripheral nerve allografts in acute rejection. *J. Neurotrauma* **18**, (2001).
56. Mackinnon, S. E., Doolabh, V. B., Novak, C. B. & Trulock, E. P. Clinical Outcome following Nerve Allograft. *Plast. Reconstr. Surg.* **107**, 1419–1429 (2001).
57. Hudson, T. W., Liu, S. Y. & Schmidt, C. E. Engineering an Improved Acellular Nerve Graft via Optimized Chemical Processing. *Tissue Eng.* **10**, 1346–1358 (2004).
58. Moore, A. M. *et al.* Acellular nerve allografts in peripheral nerve regeneration: A

comparative study. *Muscle and Nerve* (2011). doi:10.1002/mus.22033
59. Saheb-Al-Zamani, M. *et al.* Limited regeneration in long acellular nerve allografts is associated with increased Schwann cell senescence. *Exp. Neurol.* **247**, 165–177 (2013).
60. Eldridge, C. F., Bunge, M. B., Bunge, R. P. & Wood, P. M. Differentiation of axon-related Schwann cells in vitro. I. Ascorbic acid regulates basal lamina assembly and myelin formation. *J. Cell Biol.* **105**, 1023–1034 (1987).
61. Carey, D. J., Rafferty, C. M. & Todd, M. S. Effects of inhibition of proteoglycan synthesis on the differentiation of cultured rat Schwann cells. *J. Cell Biol.* **105**, 1013–1021 (1987).
62. Chernousov, M. a, Stahl, R. C. & Carey, D. J. Schwann cells use a novel collagen-dependent mechanism for fibronectin fibril assembly. *J. Cell Sci.* **111 (Pt 1**, 2763–2777 (1998).
63. Chernousov, M. a, Stahl, R. C. & Carey, D. J. Schwann cell type V collagen inhibits axonal outgrowth and promotes Schwann cell migration via distinct adhesive activities of the collagen and noncollagen domains. *J. Neurosci. Off. J. Soc. Neurosci.* **21**, 6125–6135 (2001).
64. Erdman, R., Stahl, R. C., Rothblum, K., Chernousov, M. A. & Carey, D. J. Schwann cell adhesion to a novel heparan sulfate binding site in the N-terminal domain of α4 type V collagen is mediated by syndecan-3. *J. Biol. Chem.* **277**, 7619–7625 (2002).
65. Mackinnon, S., Hudson, A., Bojanowski, V., Hunter, D. & Maraghi, E. Peripheral nerve injection injury with purified bovine collagen. *Annals of Plastic Surgery* **14**, 428–436 (1985).
66. Archibald, S. J., Krarup, C., Shefner, J., Li, S. -T & Madison, R. D. A collagen-based nerve guide conduit for peripheral nerve repair: An electrophysiological study of nerve regeneration in rodents and nonhuman primates. *J. Comp. Neurol.* **306**, 685–696 (1991).
67. Wangensteen, K. J. & Kalliainen, L. K. Collagen Tube Conduits in Peripheral Nerve Repair : A Retrospective Analysis. 273–277 (2010). doi:10.1007/s11552-009-9245-0
68. Komiyama, T. *et al.* Novel technique for peripheral nerve reconstruction in the absence of an artificial conduit. *J. Neurosci. Methods* **134**, 133–140 (2004).
69. Evans, G. R. D. *et al.* Bioactive poly(L-lactic acid) conduits seeded with Schwann cells for peripheral nerve regeneration. *Biomaterials* **23**, 841–848 (2002).
70. Bryan, D. J. *et al.* Influence of glial growth factor and Schwann cells in a bioresorbable guidance channel on peripheral nerve regeneration. *Tissue Eng.* **6**, 129–38 (2000).
71. Mackinnon, S. E. & Dellon, A. L. Clinical nerve reconstruction with a bioabsorbable polyglycolic acid tube. *Plast. Reconstr. Surg.* (1990). doi:10.1097/00006534-199003000-00015
72. Braga-Silva, J. The use of silicone tubing in the late repair of the median and ulnar nerves in the forearm. *J. Hand Surg. Am.* **24 B**, 703–706 (1999).
73. Tan, C. W. *et al.* Sciatic nerve repair with tissue engineered nerve: Olfactory ensheathing cells seeded poly(lactic-co-glygolic acid) conduit in an animal model. *Indian J. Orthop.* **47**, 547–52 (2013).
74. Schreiner, S. *et al.* Hypomorphic Sox10 alleles reveal novel protein functions and unravel developmental differences in glial lineages. *Development* **134**, 3271–3281 (2007).
75. Britsch, S. *et al.* The transcription factor Sox10 is a key regulator of peripheral glial development. *Genes Dev.* **15**, 66–78 (2001).
76. Joseph, N. M. Neural crest stem cells undergo multilineage differentiation in developing peripheral nerves to generate endoneurial fibroblasts in addition to Schwann cells. *Development* **131**, 5599–5612 (2004).

77. Dong, Z. *et al.* Neu differentiation factor is a neuron-glia signal and regulates survival, proliferation, and maturation of rat schwann cell precursors. *Neuron* **15**, 585–596 (1995).
78. Riethmacher, D. *et al.* Severe neuropathies in mice with targeted mutations in the ErbB3 receptor. *Nature* **389**, 725–730 (1997).
79. Nave, K. A. & Salzer, J. L. Axonal regulation of myelination by neuregulin 1. *Curr. Opin. Neurobiol.* **16**, 492–500 (2006).
80. Garratt, A. N., Britsch, S. & Birchmeier, C. Neuregulin, a factor with many functions in the life of a Schwann cell. *BioEssays* **22**, 987–996 (2000).
81. Michailov, G. Axonal Neuregulin-1 Regulates Myelin Sheath Thickness Galin. *Society* **296**, 1098–1101 (2002).
82. Taveggia, C. *et al.* Neuregulin-1 type III determines the ensheathment fate of axons. *Neuron* **47**, 681–694 (2005).
83. Wakamatsu, Y., Maynard, T. M. & Weston, J. A. Fate determination of neural crest cells by NOTCH-mediated lateral inhibition and asymmetrical cell division during gangliogenesis. *Development* **127**, 2811–2821 (2000).
84. Woodhoo, A. *et al.* Notch controls embryonic Schwann cell differentiation, postnatal myelination and adult plasticity. *Nat. Neurosci.* **12**, 839–847 (2009).
85. Webster, H. de F., Martin, J. R. & O'Connell, M. F. The relationships between interphase Schwann cells and axons before myelination: A quantitative electron microscopic study. *Dev. Biol.* **32**, 401–416 (1973).
86. Brennan, A. *et al.* Endothelins control the timing of Schwann cell generation in vitro and in vivo. *Dev. Biol.* **227**, 545–557 (2000).
87. Stewart, H. J. S. *et al.* Developmental regulation and overexpression of the transcription factor AP-2, a potential regulator of the timing of Schwann cell generation. *Eur. J. Neurosci.* **14**, 363–372 (2001).
88. Mirsky, R. *et al.* Novel signals controlling embryonic Schwann cell development, myelination and dedifferentiation. *J. Peripher. Nerv. Syst.* **13**, 122–135 (2008).
89. Chen, Z.-L., Yu, W.-M. & Strickland, S. Peripheral Regeneration. *Annu. Rev. Neurosci.* **30**, 209–233 (2007).
90. Jessen, K. R. & Mirsky, R. Negative regulation of myelination: Relevance for development, injury, and demyelinating disease. *Glia* **56**, 1552–1565 (2008).
91. Martinez, J. A. *et al.* Intrinsic facilitation of adult peripheral nerve regeneration by the Sonic hedgehog morphogen. *Exp. Neurol.* **271**, 493–505 (2015).
92. Boerboom, A., Dion, V., Chariot, A. & Franzen, R. Molecular Mechanisms Involved in Schwann Cell Plasticity. *Front. Mol. Neurosci.* **10**, 1–18 (2017).
93. Arthur-Farraj, P. J. *et al.* c-Jun Reprograms Schwann Cells of Injured Nerves to Generate a Repair Cell Essential for Regeneration. *Neuron* **75**, 633–647 (2012).
94. Grothe, C., Haastert, K. & Jungnickel, J. Physiological function and putative therapeutic impact of the FGF-2 system in peripheral nerve regeneration-Lessons from in vivo studies in mice and rats. *Brain Res. Rev.* **51**, 293–299 (2006).
95. Niemi, J. P. *et al.* A Critical Role for Macrophages Near Axotomized Neuronal Cell Bodies in Stimulating Nerve Regeneration. *J. Neurosci.* **33**, 16236–16248 (2013).
96. Hirata, K. & Kawabuchi, M. Myelin phagocytosis by macrophages and nonmacrophages during Wallerian degeneration. *Microsc. Res. Tech.* **57**, 541–547 (2002).
97. Rotshenker, S. Wallerian degeneration: The innate-immune response to traumatic nerve injury. *J. Neuroinflammation* **8**, (2011).

98. Jung, J. *et al.* Actin Polymerization Is Essential for Myelin Sheath Fragmentation during Wallerian Degeneration. *J. Neurosci.* **31**, 2009–2015 (2011).
99. Tofaris, G. K., Patterson, P. H., Jessen, K. R. & Mirsky, R. Denervated Schwann Cells Attract Macrophages by Secretion of Leukemia Inhibitory Factor (LIF) and Monocyte Chemoattractant Protein-1 in a Process Regulated by Interleukin-6 and LIF. *J. Neurosci.* **22**, 6696–6703 (2018).
100. Bauer, S., Kerr, B. J. & Patterson, P. H. The neuropoietic cytokine family in development , plasticity , disease and injury. **8**, 221–232 (2007).
101. Cattin, A. L. *et al.* Macrophage-Induced Blood Vessels Guide Schwann Cell-Mediated Regeneration of Peripheral Nerves. *Cell* **162**, 1127–1139 (2015).
102. Barrette, B. *et al.* Requirement of Myeloid Cells for Axon Regeneration. *J. Neurosci.* **28**, 9363–9376 (2008).
103. Gomez-Sanchez, J. A. *et al.* After Nerve Injury, Lineage Tracing Shows That Myelin and Remak Schwann Cells Elongate Extensively and Branch to Form Repair Schwann Cells, Which Shorten Radically on Remyelination. *J. Neurosci.* **37**, 9086–9099 (2017).
104. Arthur-Farraj, P. J. *et al.* Changes in the Coding and Non-coding Transcriptome and DNA Methylome that Define the Schwann Cell Repair Phenotype after Nerve Injury. *Cell Rep.* **20**, 2719–2734 (2017).
105. Painter, M. W. *et al.* Diminished Schwann cell repair responses underlie age-associated impaired axonal regeneration. *Neuron* **83**, 331–343 (2014).
106. Beck, K. D. *et al.* Mesencephalic dopaminergic neurons protected by GDNF from axotomy-induced degeneration in the adult brain. *Nature* **373**, 339–341 (1995).
107. Hoffer, B. J. *et al.* Glial cell line-derived neurotrophic factor reverses toxin-induced injury to midbrain dopaminergic neurons in vivo. *Neurosci. Lett.* **182**, 107–111 (1994).
108. Winkler, C., Sauer, H., Lee, C. S. & Björklund, A. Short-Term GDNF Treatment Provides Long-Term Rescue of Lesioned Nigral Dopaminergic Neurons in a Rat Model of Parkinson's Disease. *J. Neurosci.* **16**, 7206–7215 (1996).
109. Tomac, A. *et al.* Protection and repair of the nigrostriatal dopaminergic system by GDNF in vivo. *Nature* **373**, 335–339 (1995).
110. Arce, V. *et al.* Synergistic Effects of Schwann- and Muscle-Derived Factors on Motoneuron Survival Involve GDNF and Cardiotrophin-1 (CT-1). *J. Neurosci.* **18**, 1440–1448 (1998).
111. Poteryaev, D. *et al.* GDNF triggers a novel Ret-independent Src kinase family-coupled signaling via a GPI-linked GDNF receptor α1. *FEBS Lett.* **463**, 63–66 (1999).
112. Eketjäll, S., Fainzilber, M., Murray-Rust, J. & Ibáñez, C. F. Distinct structural elements in GDNF mediate binding to GFRα1 and activation of the GFRα1-c-Ret receptor complex. *EMBO J.* **18**, 5901–5910 (1999).
113. Tansey, M. G., Baloh, R. H., Milbrandt, J. & Johnson, E. M. GFRα-mediated localization of RET to lipid rafts is required for effective downstream signaling, differentiation, and neuronal survival. *Neuron* **25**, 611–623 (2000).
114. Ibáñez, C. F. Structure and physiology of the RET receptor tyrosine kinase. *Cold Spring Harb. Perspect. Biol.* **5**, 1–10 (2013).
115. Soler, R. M. *et al.* Receptors of the Glial Cell Line-Derived Neurotrophic Factor Family of Neurotrophic Factors Signal Cell Survival through the Phosphatidylinositol 3-Kinase Pathway in Spinal Cord Motoneurons. **19**, 9160–9169 (1999).
116. Chen, J., Chu, Y. F., Chen, J. M. & Li, B. C. Synergistic effects of NGF, CNTF and GDNF on functional recovery following sciatic nerve injury in rats. *Adv. Med. Sci.* **55**, 32–42

(2010).
117. Wood, M. D. *et al.* Affinity-based release of glial-derived neurotrophic factor from fibrin matrices enhances sciatic nerve regeneration q. *Acta Biomater.* **5**, 959–968 (2009).
118. Moore, A. M. *et al.* Controlled delivery of glial cell line-derived neurotrophic factor enhances motor nerve regeneration. *J. Hand Surg. Am.* **35**, 2008–2017 (2010).
119. Keller-Peck, C. R. *et al.* Glial cell line-derived neurotrophic factor administration in postnatal life results in motor unit enlargement and continuous synaptic remodeling at the neuromuscular junction. *J. Neurosci.* **21**, 6136–46 (2001).
120. Zwick, M., Teng, L., Mu, X., Springer, J. E. & Davis, B. M. Overexpression of GDNF induces and maintains hyperinnervation of muscle fibers and multiple end-plate formation. *Exp. Neurol.* **171**, 342–350 (2001).
121. Paratcha, G., Ledda, F. & Ibáñez, C. F. The neural cell adhesion molecule NCAM is an alternative signaling receptor for GDNF family ligands. *Cell* **113**, 867–879 (2003).
122. Iwase, T., Jung, C. G., Bae, H., Zhang, M. & Soliven, B. Glial cell line-derived neurotrophic factor-induced signaling in Schwann cells. *J. Neurochem.* **94**, 1488–1499 (2005).
123. Jesuraj, N. J., Marquardt, L. M., Kwasa, J. A. & Sakiyama-Elbert, S. E. Glial cell line-derived neurotrophic factor promotes increased phenotypic marker expression in femoral sensory and motor-derived Schwann cell cultures. *Exp. Neurol.* **257**, 10–18 (2014).
124. Höke, A. *et al.* Glial cell line-derived neurotrophic factor alters axon schwann cell units and promotes myelination in unmyelinated nerve fibers. *J. Neurosci.* **23**, 561–567 (2003).
125. Jesuraj, N. J. *et al.* Differential gene expression in motor and sensory Schwann cells in the rat femoral nerve. *J. Neurosci. Res.* **90**, 96–104 (2012).
126. Marquardt, L. M. & Sakiyama-Elbert, S. E. GDNF preconditioning can overcome Schwann cell phenotypic memory. *Exp. Neurol.* **265**, 1–7 (2015).
127. Dittrich, F. *et al.* Pharmacokinetics of Intrathecally Applied BDNF and Effects on Spinal Motoneurons. **239**, 225–239 (1996).
128. Anderson, K. D. *et al.* Differential Distribution of Exogenous BDNF , NGF , and NT-3 in the Brain Corresponds to the Relative Abundance and Distribution of High-Affinity and Low-Affinity Neurotrophin Receptors. **317**, (1995).
129. Allodi, I. *et al.* Schwann Cells Transduced with a Lentiviral Vector Encoding Fgf-2 Promote Motor Neuron Regeneration Following Sciatic Nerve Injury. (2014). doi:10.1002/glia.22712
130. Eggers, R. *et al.* Lentiviral Vector-Mediated Gradients of GDNF in the Injured Peripheral Nerve: Effects on Nerve Coil Formation, Schwann Cell Maturation and Myelination. *PLoS One* **8**, (2013).
131. Eggers, R. *et al.* Molecular and Cellular Neuroscience Neuroregenerative effects of lentiviral vector-mediated GDNF expression in reimplanted ventral roots. **39**, 105–117 (2008).
132. Shakhbazau, A. *et al.* Doxycycline-regulated GDNF expression promotes axonal regeneration and functional recovery in transected peripheral nerve. *J. Control. Release* **172**, 841–851 (2013).
133. Ginhoux, F. *et al.* HLA-A * 0201-Restricted Cytolytic Responses to the rtTA Transactivator Dominant and Cryptic Epitopes Compromise Transgene Expression Induced by the Tetracycline on System. *Mol. Ther.* **10**, 279–289 (2004).
134. Markusic, D. M., Waart, D. R. De & Seppen, J. Separating Lentiviral Vector Injection and Induction of Gene Expression in Time , Does Not Prevent an Immune Response to rtTA in

Rats. **5**, (2010).
135. Favre, D. *et al.* Lack of an Immune Response against the Tetracycline-Dependent Transactivator Correlates with Long-Term Doxycycline-Regulated Transgene Expression in Nonhuman Primates after Intramuscular Injection of Recombinant Adeno-Associated Virus. **76**, 11605–11611 (2002).
136. Latta-mahieu, M. *et al.* Gene Transfer of a Chimeric Trans-Activator Is Immunogenic and Results in Short-Lived Transgene Expression. **1620**, 1611–1620 (2002).
137. Guiner, C. Le *et al.* Transgene Regulation Using the Tetracycline-Inducible TetR-KRAB System after AAV-Mediated Gene Transfer in Rodents and Nonhuman Primates. **9**, (2014).
138. Eggers, R. *et al.* Timed GDNF gene therapy using an immune-evasive gene switch promotes long distance axon regeneration. 295–311 (2019). doi:10.1093/brain/awy340
139. Fox, I. K. *et al.* Schwann-cell injection of cold-preserved nerve allografts. *Microsurgery* **25**, 502–507 (2005).
140. Moore, A. M., Ray, W. Z., Chenard, K. E., Tung, T. & Mackinnon, S. E. Nerve allotransplantation as it pertains to composite tissue transplantation. *Hand* **4**, 239–244 (2009).
141. Kobayashi, J. *et al.* The effect of duration of muscle denervation on functional recovery in the rat model. *Muscle Nerve* **20**, 858–66 (1997).
142. Siddique, R. & Thakor, N. Investigation of nerve injury through microfluidic devices. *J. R. Soc. Interface* **11**, 20130676 (2014).
143. Park, J. W., Vahidi, B., Taylor, A. M., Rhee, S. W. & Jeon, N. L. Microfluidic culture platform for neuroscience research. *Nat. Protoc.* **1**, 2128–36 (2006).
144. Taylor, A. M. *et al.* A microfluidic culture platform for CNS axonal injury, regeneration and transport. *Nat. Methods* **2**, 599–605 (2005).
145. Cohen, M. S., Orth, C. B., Kim, H. J., Jeon, N. L. & Jaffrey, S. R. Neurotrophin-mediated dendrite-to-nucleus signaling revealed by microfluidic compartmentalization of dendrites. *Proc. Natl. Acad. Sci. U. S. A.* **108**, 11246–11251 (2011).
146. Tao, Y. Isolation and culture of Schwann cells. *Methods in molecular biology (Clifton, N.J.)* **1018**, 93–104 (2013).
147. Batchelor, P. Macrophages and Microglia Produce Local Trophic Gradients That Stimulate Axonal Sprouting Toward but Not beyond the Wound Edge. *Mol. Cell. Neurosci.* **21**, 436–453 (2002).
148. Lin, Y.-C. *et al.* Spatially controlled delivery of neurotrophic factors in silk fibroin-based nerve conduits for peripheral nerve repair. *Ann. Plast. Surg.* **67**, 147–155 (2011).
149. Tannemaat, M. R., Boer, G. J., Verhaagen, J. & Malessy, M. J. A. Genetic modification of human sural nerve segments by a lentiviral vector encoding nerve growth factor. *Neurosurgery* **61**, 1286–1294 (2007).
150. Kells, A. P. *et al.* AAV-mediated gene delivery of BDNF or GDNF is neuroprotective in a model of Huntington disease. *Mol. Ther.* **9**, 682–688 (2004).
151. Garbayo, E. *et al.* Effective GDNF brain delivery using microspheres-A promising strategy for Parkinson's disease. *J. Control. Release* **135**, 119–126 (2009).
152. Madduri, S., Feldman, K., Tervoort, T., Papaloïzos, M. & Gander, B. Collagen nerve conduits releasing the neurotrophic factors GDNF and NGF. *J. Control. Release* **143**, 168–174 (2010).
153. Tolwani, R. J. *et al.* BDNF overexpression produces a long-term increase in myelin formation in the peripheral nervous system. *J. Neurosci. Res.* **77**, 662–669 (2004).

154. Albers, K. M., Wright, D. E. & Davis, B. M. Overexpression of nerve growth factor in epidermis of transgenic mice causes hypertrophy of the peripheral nervous system. *J. Neurosci.* **14**, 1422–1432 (1994).
155. Albers, K. M. *et al.* Cutaneous overexpression of NT-3 increases sensory and sympathetic neuron number and enhances touch dome and hair follicle innervation. *J. Cell Biol.* **134**, 487–497 (1996).
156. Ee, X. *et al.* Transgenic SCs expressing GDNF-IRES-DsRed impair nerve regeneration within acellular nerve allografts. *Biotechnol. Bioeng.* **114**, 2121–2130 (2017).
157. Mohajeri, M. H., Figlewicz, D. A. & Bohn, M. C. Intramuscular grafts of myoblasts genetically modified to secrete glial cell line-derived neurotrophic factor prevent motoneuron loss and disease progression in a mouse model of familial amyotrophic lateral sclerosis. *Hum. Gene Ther.* **10**, 1853–66 (1999).
158. Koliatsos, V. E. *et al.* Ventral Root Avulsion: **44**, (1994).
159. Sulaiman, O. A. R., Ph, D., Gordon, T. & Ph, D. CELLULAR AND MOLECULAR CHANGES. **65**, 105–114 (2009).
160. Jonsson, S. *et al.* Effect of Delayed Peripheral Nerve Repair on Nerve Regeneration , Schwann Cell Function and Target Muscle Recovery. **8**, (2013).
161. Ronchi, G. *et al.* Irreversible changes occurring in long-term denervated Schwann cells affect delayed nerve repair. **127**, 843–856 (2017).
162. Jessen, K. R. & Mirsky, R. The repair Schwann cell and its function in regenerating nerves. *J. Physiol.* **594**, 3521–3531 (2016).
163. Heumann, R. *et al.* Differential Regulation of mRNA Encoding Nerve Growth Factor and Its Receptor in Rat Sciatic Nerve during Development , Degeneration , and Regeneration : Role of Macrophages Radeke , Thomas P . Misko , Eric Shooter and Hans Thoenen Source : Proceedings of. (1987).
164. Naveilhan, P., EiShamy, W. M. & Ernfors, P. Differential regulation of mRNAs for GDNF and its receptors Ret and GDNFRα after sciatic nerve lesion in the mouse. *Eur. J. Neurosci.* **9**, 1450–1460 (1997).
165. Meyer, M. & Matsuoka, I. Enhanced Synthesis of Brain-derived Neurotrophic Factor in the Lesioned Peripheral Nerve: Different Mechanisms Are Responsible for the Regulation of BDNF and NGF mRNA. **119**, 45–54 (1992).
166. Funakoshi, H. *et al.* Differential Expression of mRNAs for Neurotrophins and Their Receptors after Axotomy of the Sciatic Nerve. **123**, 455–465 (1993).
167. Hoke, A., Cheng, C. & Zochodne, D. W. Expression of glial cell line-derived neurotrophic factor family of growth factors in peripheral nerve injury in rats. **11**, 1651–1654 (2000).
168. Sakamoto, T. *et al.* Adenoviral Gene Transfer of GDNF , BDNF and TGF ᴺʟ 2 , but not CNTF , Cardiotrophin-1 or IGF1 , Protects Injured Adult Motoneurons After Facial Nerve Avulsion. **64**, 54–64 (2003).
169. Wood, M. D., Borschel, G. H. & Sakiyama-elbert, S. E. Controlled release of glial-derived neurotrophic factor from fibrin matrices containing an affinity-based delivery system. (2008). doi:10.1002/jbm.a.32043
170. Morgan, L., Jessen, K. R. & Mirsky, R. The effects of cAMP on differentiation of cultured schwann cells: Progression from an early phenotype (04+) to a myelin phenotype (P○+, GFAP-, N-CAM-, NGF-receptor-) depends on growth inhibition. *J. Cell Biol.* **112**, 457–467 (1991).
171. Klemke, R. L. *et al.* Regulation of cell motility by mitogen-activated protein kinase. *J. Cell*

Biol. **137**, 481–492 (1997).
172. Meintanis, S., Thomaidou, D., Jessen, K. R., Mirsky, R. & Matsas, R. The neuron-glia signal beta-neuregulin promotes Schwann cell motility via the MAPK pathway. *Glia* **34**, 39–51 (2001).
173. Hadaczek, P., Johnston, L., Forsayeth, J. & Bankiewicz, K. S. Neuropharmacology Pharmacokinetics and bioactivity of glial cell line-derived factor (GDNF) and neurturin (NTN) infused into the rat brain. *Neuropharmacology* **58**, 1114–1121 (2010).
174. Wang, Z. Z., Wood, M. D., Mackinnon, S. E. & Sakiyama-Elbert, S. E. A Microfluidic Platform to Study the Effects of GDNF on Neuronal Axon Entrapment. *J. Neurosci. Methods* **308**, 183–191 (2018).
175. Wang, Z. Z., Wood, M. D., Mackinnon, S. E. & Sakiyama-Elbert, S. E. A Microfluidic Platform to Study the Effects of GDNF on Neuronal Axon Entrapment. *J. Neurosci. Methods* **308**, 183–191 (2018).
176. Schmittgen, T. D. & Livak, K. J. Analyzing real-time PCR data by the comparative C(T) method. *Nat. Protoc.* (2008).
177. Nichols, C. M. *et al.* Effect of motor versus sensory nerve grafts on peripheral nerve regeneration. *Exp. Neurol.* **190**, 347–355 (2004).
178. Fang, X. *et al.* GDNF pretreatment overcomes Schwann cell phenotype mismatch to promote motor axon regeneration via sensory graft. *Exp. Neurol.* **318**, 258–266 (2019).
179. Aruga, J. & Mikoshiba, K. Identification and characterization of Slitrk, a novel neuronal transmembrane protein family controlling neurite outgrowth. *Mol. Cell. Neurosci.* **24**, 117–129 (2003).
180. Gatto, G. *et al.* Protein tyrosine phosphatase receptor type O inhibits trigeminal axon growth and branching by repressing TrkB and ret signaling. *Ann. Intern. Med.* (2013). doi:10.1523/JNEUROSCI.4707-12.2013
181. Proenca, C. C., Gao, K. P., Shmelkov, S. V, Rafii, S. & Lee, F. S. Slitrks as emerging candidate genes involved in neuropsychiatric disorders. *Trends Neurosci.* **34**, 143–153 (2011).
182. Um, J. W. & Ko, J. LAR-RPTPs : synaptic adhesion molecules that shape synapse development. *Trends Cell Biol.* **23**, 465–475 (2013).
183. Batchelor, P. E. *et al.* Macrophages and microglia produce local trophic gradients that stimulate axonal sprouting toward but not beyond the wound edge. *Mol. Cell. Neurosci.* **21**, 436–453 (2002).
184. Jesuraj, N. J. *et al.* Schwann cells seeded in acellular nerve grafts improve functional recovery. *Muscle and Nerve* **49**, 267–276 (2014).
185. Magill, C. K. *et al.* The differential effects of pathway- versus target-derived glial cell line–derived neurotrophic factor on peripheral nerve regeneration. **113**, 102–109 (2010).
186. Abelson, J. F. *et al.* Sequence Variants in SLITRK1 Are Associated with Tourette ' s Syndrome Published by : American Association for the Advancement of Science Stable URL : https://www.jstor.org/stable/3842662 REFERENCES Linked references are available on JSTOR for this articl. *Science (80-.).* **310**, 317–320 (2005).
187. Shmelkov, S. V *et al.* Slitrk5 deficiency impairs corticostriatal circuitry and leads to obsessive-compulsive – like behaviors in mice. *Nat. Med.* **16**, 598–602 (2010).
188. Katayama, K. *et al.* Disorganized Innervation and Neuronal Loss in the Inner Ear of Slitrk6-Deficient Mice. **4**, 1–13 (2009).
189. Mandai, K. *et al.* LIG Family Receptor Tyrosine Kinase-Associated Proteins Modulate

Growth Factor Signals during Neural Development. *Neuron* **63**, 614–627 (2009).
190. Takahashi, H. *et al.* Selective control of inhibitory synapse development by Slitrk3-PTP d trans-synaptic interaction. *Nat. Publ. Gr.* **15**, 389–398 (2012).
191. Shin, Y. *et al.* Slitrks control excitatory and inhibitory synapse formation with LAR receptor protein tyrosine phosphatases. 2–7 (2012). doi:10.1073/pnas.1209881110
192. Jiang, W. *et al.* Identification of Protein Tyrosine Phosphatase Receptor Type O (PTPRO) as a Synaptic Adhesion Molecule that Promotes Synapse Formation. **37**, 9828–9843 (2017).
193. Ledda, F., Paratcha, G., Sandoval-Guzmán, T. & Ibáñez, C. F. GDNF and GFRalpha1 promote formation of neuronal synapses by ligand-induced cell adhesion. *Nat. Neurosci.* **10**, 293–300 (2007).
194. Parrinello, S. *et al.* EphB signaling directs peripheral nerve regeneration through Sox2-dependent Schwann cell Sorting. *Cell* **143**, 145–155 (2010).
195. Nguyen, Q. T., Parsadanian, A. S., Snider, W. D. & Lichtman, J. W. Hyperinnervation of neuromuscular junctions caused by GDNF overexpression in muscle. *Science (80-.).* (1998). doi:10.1126/science.279.5357.1725
196. Yan, Y., Sun, H. H., Mackinnon, S. E. & Johnson, P. J. Evaluation of peripheral nerve regeneration via in vivo serial transcutaneous imaging using transgenic Thy1-YFP mice. *Exp. Neurol.* (2011). doi:10.1016/j.expneurol.2011.06.013
197. Esper, R. M. Rapid Axoglial Signaling Mediated by Neuregulin and Neurotrophic Factors. *J. Neurosci.* (2004). doi:10.1523/JNEUROSCI.1692-04.2004

Vita

Ze Zhong Wang

Education

Washington University in St. Louis, Saint Louis MO August 2013 – August 2019
Ph.D., Biomedical Engineering Expected August 2019
M.S., Biomedical Engineering May 2016

University of California, San Diego, San Diego, CA September 2008 – June 2013
B.S., Bioengineering – Biotechnology

Research Experience

Washington University in St. Louis, Biomedical Engineering 2013-2019
Doctoral Research Student, Mentor: Prof. Shelly Sakiyama-Elbert, Ph.D.

Thesis: A Microfluidic Platform to Investigate the Mechanism by which GDNF Overexpression in Schwann Cells Causes Neuronal Axon Entrapment

- Developed a microfluidic device that models neuronal axon entrapment caused by high GDNF concentrations.
- Studied the mechanism by which GDNF causes axon entrapment.

University of California, San Diego, Medicine and Bioengineering 2011-2013
Ideker Laboratory, Prof. Trey Ideker, Ph.D.

- Examine the effects of common human analogue of tumor suppressor gene mutations in Saccharomyces cerevisiae, perform large scale screening of double mutant, and by conducting experiments focused on chemotherapeutic agents and gene interactions

University of British Columbia, Biochemistry and Molecular Biology 2007-2009
Bromme Laboratory, Prof. Dieter Bromme, Ph.D

- Examined excessive proteolytic degradation diseases such as atherosclerosis and cartilage diseases by collecting alveoli tissues from laboratory mice and using Western Blotting

Publications

1. **Wang, Z**., Wood, M., Mackinnon, S., and Sakiyama-Elbert, S. (2018). A microfluidic platform to study the effects of GDNF on neuronal axon entrapment. *Journal of Neuroscience Methods*, 308, pp.183-191.
2. **Wang, Z.,** and Sakiyama-Elbert, S. (2019). Matrices, scaffolds & carriers for cell delivery in nerve regeneration. *Experimental Neurology*, 319, p.112837.

3. **Wang, Z.**, Wood, M., Mackinnon, S., and Sakiyama-Elbert, S. Slitrk4 Activation by High GDNF Levels Leads to Neuronal Axon Entrapment. (In preparation).
4. Guénolé, A., Srivas, R., Vreeken, K., Wang, **Z., Wang**, S., Krogan, N., Ideker, T., and van Attikum, H. (2013). Dissection of DNA Damage Responses Using Multiconditional Genetic Interaction Maps. *Molecular Cell*, 49(2), pp.346-358.

Conference Presentations

Oral Presentations

1. **Wang, Z**., Wood, M., Mackinnon, S. and Sakiyama-Elbert, S. A Microfluidic Platform to Study the Effects of GDNF on Neuronal Axon Entrapment. Biomedical Engineering Society Annual Conference. October 2017.

Poster Presentations

1. **Wang, Z**., Wood, M., Mackinnon, S. and Sakiyama-Elbert, S. A Microfluidic Platform to Study the Effects of GDNF on Neuronal Axon Entrapment. Tissue Engineering and Regenerative Medicine International Society-Americas. December 2016.